Calculation of phase equilibria of quantum fluids at high pressure

Rozita Laghaei

aus Teheran, Iran

April 23, 2003

to my parents and to Afshin,
whose patience and love enabled me
to complete this work.

Acknowledgements

I am deeply indepted to my supervisor Prof. Dr. U. K. Deiters whose help and encouragement gave me the possibility to complete this thesis.

I would like to express my gratitude to Prof. Dr. R. Strey whose support and advice was great help in difficult times and enabled me to complete this work.

Contents

1

List of Figures

List of Tables

Abstract

The thermodynamic properties of liquids or compressed gases of light atoms and molecules show deviations from classical predictions. These light molecules does not obey the corresponding states principle. The observed deviations are caused by so-called quantum effects.

The quantum effects are due to the two main reasons. First, the discontinuity of the energy levels at very high densities, when the motions of particles are restricted (by the boundary conditions), and second, as a result of the wave function symmetry effects, which occurs at very low temperature (when only the number of particles allowed to share a quantum state becomes important).

A quantum correction proposed by Deiters [53-54] is based on the assumption that each molecule is restricted to a cubic cell with a size depending on the free volume. This model is a straightforward and easy method for prediction of thermodynamic properties of quantum fluids at high densities. However, the cell model is not suitable at low densities or high temperatures, and the cubic form of the cell (which is applied for mathematical convenience) is not a realistic assumption.

In the present work the quantum effects are considered by means of a more realistic "spherical cell model". This quantum correction can be applied to any van der Waals type equation of state. A correction function has been developed to overcome the weaknesses of the cell model at low density or high temperature limit. The corrections are applied to the Deiters equation of state [50, 51, 52], and the phase equilibria for pure quantum fluids and binary mixtures are calculated. Calculations have been made for the pure fluids hydrogen, neon, methane, and nitrogen as well

9

as, for the binary mixtures neon–argon and neon–krypton. The results of the spherical cell model for all cases show significant improvement in comparison with the cubic cell model results.

Zusammenfassung

Die thermodynamischen Eigenschaften von Flüssigkeiten oder komprimierten Gasen, die aus leichten Atomen oder Molekülen bestehen, weisen Abweichungen von den klassischen Vorhersagen auf. Diese Moleküle gehorchen nicht dem Prinzip der korrespondierenden Zustände. Die beobachteten Abweichungen werden von sogenannten Quanteneffekten verursacht.

Quanteneffekte lassen sich auf zwei Ursachen zurückführen: erstens auf die Diskontinuität der Energieniveaus bei sehr hohen Dichten, wenn die Bewegungen der Moleküle eingeschränkt sind (durch Randbedingungen), und zweitens auf Symmetrieeffekte der Wellenfunktionen, die bei sehr niedrigen Temperaturen auftreten (wenn nur ist die Zahl der Moleküle wichtig, die sich einen Quantenzustand teilen können).

Eine von Deiters [53-54] vorgeschlagene Quantenkorrektur beruht auf der Annahme, jedes Molekül sei auf eine kubische Zelle beschränkt, deren Größe vom freien Volumen abhängt. Dieses Modell ist eine direkte und einfache Methode zur Abschätzung der thermodynamischen Eigenschaften von Quantenfluiden bei hohen Dichten. Allerdings eignet sich das Modell nicht für niedrige Dichte oder hohe Temperaturen, und die kubische Zellengestalt (die nur wegen der mathematischen Einfachheit gewählt wurde) ist keine realistische Annahme.

In dieser Arbeit werden Quanteneffekte mit Hilfe eines realistischeren "sphärischen Zellenmodells" beschrieben. Diese Quantenkorrektur kann auf jede Zustandsgleichung von Van-der-Waals-Typ angewandt werden. Um die Schwäche der Zellenmodelle bei niedrigen Dichten oder hohen Temperaturen auszugleichen wurde eine Korrekturfunktion entwickelt.

Die Korrekturen wurden auf die Zustandsgleichung von Deiters [50, 51,

52] angewandt und damit Phasengleichgewichte reiner Quantenfluide und binärer Mischungen berechnet. Es wurden Rechnungen durchgeführt für die reinen Fluide Wasserstoff, Neon, Methan und Stickstoff sowie für die binären Mischsysteme Neon–Argon und Neon–Krypton. Die unter Verwendung des sphärischen Zellenmodells erzielten Resultate zeigen in allen Fällen eine deutliche Verbesserung im Vergleich zum kubischen Zellenmodell.

Chapter 1

Introduction

For the understanding of fundamentals of industrial processes such as designing and optimizing of separation processes, purification processes to obtain high purity compounds or mixtures of constant composition, etc. the knowledge of phase equilibria is necessary.

For systems containing one or more substances, the representation of phase equilibria can be obtained when the functional relation between temperature, pressure, volume and phase composition is known.

One of the most useful methods for the calculation of phase equilibria is based on equations of state. The equation of state method uses a homogeneous model for all fluid phases and is in principle applicable to pure substances and mixtures.

A very powerful tool available to predict the properties of fluids and fluid mixtures is the corresponding states principle. From this corresponding states principle, and a knowledge of few reference systems, fluid properties can be predicted with a minimum information. The corresponding states theory was first proposed by van der Waals, who derived it for his equation of state.

The simple corresponding states theory is based on three assumptions:

1. The potential energy function is the same for all substances, and is a function of the energy and distance characteristic parameters of the substance.

2. The canonical partition function can be separated into two independent parts, a translational part, and an internal part.

3. The translational part of the partition function can be evaluated classically, and classical statistics (Boltzmann statistics) can be used.

When one or more of the above assumptions are not valid, deviations occur in the simple corresponding states principle.

The first assumption that the potential is a universal function of the two parameters (energy and distance) to characterize a molecule, is a good approximation for simple molecules. For more complex molecules such as polar and polyatomic fluids additional parameters are needed.

Assumption 2 may be in error for solids, and may have some error if used for polyatomic fluids at high densities.

The assumptions 1 and 2 must be obeyed completely by the monoatomic and very simple molecules. In fact, the simple corresponding states is closely obeyed by argon, krypton and xenon, however, very light molecules H_2, He, and Ne are exceptions. This deviation is due to the nonvalidity of the third assumption because of the non negligible quantum effects. These quantum effects can be due to either the discontinuity of the energy levels, or the symmetry effects of the wave functions. The first category appears when the motions of particles are restricted (by the boundary conditions) and occur at high densities (when the intermolecular distances are comparable with the de Broglie wavelength). The second category occurs at very low temperature when the lowest energy levels are occupied and several particles being in one orbital state. In this case, the Boltzmann statistics is no longer applicable and Bose–Einstein or Fermi–Dirac statistics must be applied. The term Λ^*

$$\Lambda^* = \frac{h}{\sigma \sqrt{m\epsilon}} \tag{1.1}$$

is a measure of the quantum effects. In this equation m is mass of the particle, h is Planck's constant, and ϵ and σ are characteristic parameters for interaction energy and distance respectively. In the classical limit, the term Λ^* vanishes and the third assumption becomes valid. Table 1.1 shows some atoms and molecules, and their corresponding Λ^* [8].

Addition of quantum corrections to the equations of state can extend their applicability to a wider range of temperatures, pressures, and a larger variety of molecules.

Several attempts have been made to calculate the quantum effects on equilibrium properties of fluids. Some of them have been based on the virial expansion, and perturbation theory (see e.g., [58, 59]). This approach is good for weakly quantized fluids at low density, but hard sphere perturbation series may not even converge at high density. Other attempts have been based on the concept of restriction of translational motion of molecules to a cell composed of the surrounding molecules, e.g., the quantized Lennard–Jones–Devonshire cell theory of Hamann [60, 61], Levelt and Hurst [62], and Hooper and Nordholm [63]. However, their results are not good in the classical limit because they reduce to the unsuitable

substance	Λ^*
He	2.59
H_2	1.72
Ne	0.58
N_2	0.23
CH_4	0.23
Ar	0.18
Kr	0.10
CF_4	0.08
Xe	0.06
SF_6	0.04
$C(CH_3)$	0.05

Table 1.1: The measure of quantum effects for some substances.

equations of state in that limit.

A method proposed by Deiters [53, 54] which is based on the assumption that each molecule is restricted to a cell with a size depending on the free volume. Deiters approximated a cubic cell for computational convenience. The results are applicable for any van der Waals type equation of state (which is defined as an equation of state that its repulsion and attraction terms are separable). This model is a good method for prediction of thermodynamic properties of quantum fluids at high densities. However, the assumption of cubic cells is unrealistic, furthermore, the cell model is not suitable at low densities or high temperatures.

The present work aims at developing a quantum correction that is applicable over the full range of fluid densities, and to overcome the over simplifications of the cubic cell models.

The material of Chapter 2 introduces the concept of quantum mechanics. Some models which are used throughout this work are presented. Chapter 3 is a review in statistical mechanics, emphasizes the methods of the canonical partition function and its factorization. The results of this

chapter are used in of the following chapters. Chapter 4 contains a short review in equations of state and mixing rules, with emphasise on an equation of state which is applied as a reference equation in the next chapter. In Chapter 5, new correction functions are developed for van der Waals type equations of state over a wide range of temperatures and densities. In Chapter 6, the results of applying the new correction functions to the equation of state are given.

Chapter 2

Quantum Mechanics

2.1 Introduction

To calculate the macroscopic properties of matter which are also called bulk properties theoretically, we need to know about

1. the proper microstates to perform the averages.

2. the proper method for computing the average that corresponds to the bulk property.

The mathematical solution of the formulas of quantum mechanics provide the microscopic or molecular energy values. From these energy levels, the methods of statistical mechanics can be applied to calculate the observable or macroscopic properties of a system.

Atomic or Molecular model → (quantum mechanics) → Microscopic or quantum energy states of the model system → (statistical mechanics) → Bulk or macroscopic properties of system
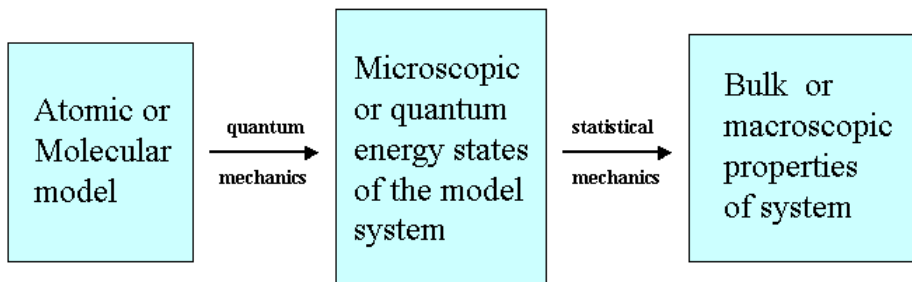
2.2   Matter waves and the Schrödinger equation

Experiments, particularly scattering of electrons and atoms, show that matter can not be completely localized on the microscopic scale [1] . Each bit of matter is associated with a kind of field, Ψ, which has a wavelike character. The wavelength of these waves is given by the de Broglie equation in free space

$$\Lambda = \frac{h}{mv} \tag{2.1}$$

where Λ is the de Broglie wavelength, h is Planck's constant, m is the mass, and v is the velocity of the particle. The behaviour of the particle is predictable only if the Ψ-waves are known. The entity $\mid \Psi^2 \mid$ (more accurately, $\Psi^*\Psi$, where Ψ^* is the complex conjugate of Ψ) is the only entity connection between the macroscopic world and microscopic world. A rigorous formalism of quantum mechanics was first developed by Werner Heisenberg (1901-1976), an equivalent form discovered by Erwin Schrödinger (1887-1961) independently.

The classical mechanical variables (x, y, z for coordinates, p_x, p_y and p_z for the momentum components, E for the total energy, etc.) are converted into mathematical operators in quantum mechanics by a set of rules (x, y, z for the coordinates, $\hbar/i(\partial/\partial x), \hbar/i(\partial/\partial y)$ and $\hbar/i(\partial/\partial z)$ for the momentum components and $-\hbar/i(\partial/\partial t)$ for the energy, etc.). These operators act on the wave function Ψ. The classical total energy is given by

$$\frac{1}{2m}(p_x^2 + p_y^2 + p_z^2) + V(x, y, z) = E \tag{2.2}$$

By substitution of the operators and by insertion of the operand $\Psi(x, y, z)$ into Eqn. 2.2 it is converted into the time-dependent Schrödinger equation

$$-\frac{\hbar^2}{2m}\Big(\frac{\partial^2}{\partial x^2} + \frac{\partial^2}{\partial y^2} + \frac{\partial^2}{\partial z^2}\Big)\Psi(x, y, z, t) + V(x, y, z)\Psi = -\frac{\hbar}{i}\frac{\partial\Psi(x, y, z, t)}{\partial t} \tag{2.3}$$

21

2.3 The time-independent Schrödinger equation

The Eqn. 2.3 can be separated into two parts, one a function of x, y, z and the other a function of t

$$\Psi = \psi(x,y,z) \ \phi(t) \tag{2.4}$$

Substitution of this equation into Eqn. 2.3 and dividing by $\psi(x,y,z) \ \phi(t)$ gives

$$\frac{1}{\psi}\left\{ -\frac{\hbar^2}{2m}\Big(\frac{\partial^2}{\partial x^2} + \frac{\partial^2}{\partial y^2} + \frac{\partial^2}{\partial z^2}\Big)\psi + V(x,y,z)\psi \right\} = -\frac{\hbar}{i}\frac{1}{\phi(t)}\frac{\mathrm{d}\phi(t)}{\mathrm{d}t} \tag{2.5}$$

The right side of Eqn. 2.5 is a function of time and the left side is a function of coordinates only. This equation is only valid if each side is equal to some constant which is called E. Thus we obtain

$$\frac{\mathrm{d}\phi(t)}{\mathrm{d}t} = -\frac{i}{\hbar}E\phi(t) \tag{2.6}$$

The Eqn. 2.6, which is only time dependent, has the solution

$$\phi(t) = \mathrm{e}^{-iEt/\hbar} \tag{2.7}$$

Equating the the left side of the Eqn. 2.5 to E, we obtain

$$-\frac{\hbar^2}{2m}\Big(\frac{\partial^2}{\partial x^2} + \frac{\partial^2}{\partial y^2} + \frac{\partial^2}{\partial z^2}\Big)\psi + V(x,y,z)\psi = E\psi \tag{2.8}$$

Eqn. 2.8 is the time-independent Schrödinger equation for a single particle of mass m. E has the same dimensions as V, and is the energy of the system. If the potential energy is a function of the coordinates only, the wave function is of the form

$$\Psi = \mathrm{e}^{-iEt/\hbar} \ \psi(x,y,z) \tag{2.9}$$

22

2.4 The symmetry of wave functions

In quantum mechanics we can not follow the exact path of a quantum particle. If the particles are all identical, there is no way to distinguish between the particles. A system of N identical particles is described by a wave function $\psi(1, 2, 3, ..., N)$. If we exchange two particles, there are two possible cases for the wave function of the system: it must remain the same (symmetric) or change its sign (antisymmetric) [6].

For particles with an integral spin (e.g., the He-4 nucleus, photons, ...), which are called bosons, the wave function is symmetric. For particles with half-integral spin (e.g., electrons, ...), which are called fermions, the wave function is antisymmetric.

2.5 The particle in a cubic box

We consider a particle in a three dimensional cubic box with edges of length R_0 (see Fig. 2.1), where the potential energy function can be expressed as follows

$$V(x, y, z) = \begin{cases} 0 & \text{for} < x, y, z < R_0 \\ \infty & \text{elsewhere} \end{cases}$$

The wave function must be zero outside the box because the particle can not have infinite energy.

The Schrödinger equation for this system is

$$-\frac{\hbar^2}{2m}\Big(\frac{\partial^2\psi}{\partial x^2} + \frac{\partial^2\psi}{\partial y^2} + \frac{\partial^2\psi}{\partial z^2}\Big) = E\psi \tag{2.10}$$

We assume that ψ is the product of three functions, each dependent upon only one variable.

$$\psi(x, y, z) = X(x)Y(y)Z(z) \tag{2.11}$$

Substituting this expression into 2.10 and dividing by $X(x)Y(y)Z(z)$, we have

$$\frac{\hbar^2}{2m}\frac{1}{X(x)}\frac{\mathrm{d}^2X(x)}{\mathrm{d}x^2} + \frac{\hbar^2}{2m}\frac{1}{Y(y)}\frac{\mathrm{d}^2Y(y)}{\mathrm{d}y^2} + \frac{\hbar^2}{2m}\frac{1}{Z(z)}\frac{\mathrm{d}^2Z(z)}{\mathrm{d}z^2} = -E \quad (2.12)$$

Each of the three parts in the left side of Eqn. 2.12 must be equal to a constant. Since the Eqn. 2.12 must be valid for all values of the three independent variables x, y,and z,

$$\frac{\mathrm{d}^2 X(x)}{\mathrm{d}x^2} + \frac{2m}{\hbar^2} E_x X(x) = 0$$
$$\frac{\mathrm{d}^2 Y(y)}{\mathrm{d}y^2} + \frac{2m}{\hbar^2} E_y Y(y) = 0$$
$$\frac{\mathrm{d}^2 Z(z)}{\mathrm{d}z^2} + \frac{2m}{\hbar^2} E_z Z(z) = 0 \tag{2.13}$$

where $E_x + E_y + E_z = E$.

Now we have three separated ordinary differential equations. This is possible because the fact that $V(x, y, z)$ is a sum of terms each dependent upon only one of the three space variables. According to the usual postulates, ψ and its partial derivatives must be continuous, finite and single valued for all values of x, y and z, and ψ must be "square integrable",
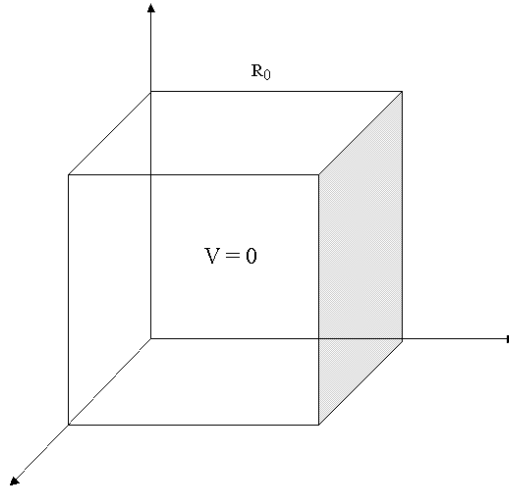
Figure 2.1: Potential energy model for Eqn. 2.5 .

or

$$\int_{-\infty}^{\infty} \psi^* \psi \, \mathrm{d}x \mathrm{d}y \mathrm{d}z = 1 \qquad (2.14)$$

it means that $\psi^* \psi$ is normalized. If the potential "walls" are infinite (an idealization), then $X(x), Y(y)$ and $Z(z)$ must vanish at the boundaries. Then we can obtain the eigenvalues and eigenfunctions

$$X(x) = \sqrt{\frac{2}{R_0}} \sin \frac{n_x \pi x}{R_0} \qquad 0 \leqslant \mathrm{x} \leqslant R_0 \qquad (2.15)$$

$$E_x = \frac{n_x^2 \hbar^2 \pi^2}{2m R_0^2} \qquad (2.16)$$

we therefore, obtain from 2.11

$$\psi = \sqrt{\frac{8}{R_0}} \sin \frac{n_x \pi x}{R_0} \sin \frac{n_y \pi y}{R_0} \sin \frac{n_z \pi z}{R_0} \qquad (2.17)$$

where n_x, n_y and n_z are independent and may have the values 1, 2, 3, 4, ... and

$$E = \frac{(n_x^2 + n_y^2 + n_z^2)\hbar^2 \pi^2}{2m R_0^2} \qquad (2.18)$$

or

$$E = \frac{(n_x^2 + n_y^2 + n_z^2)h^2}{8m R_0^2} \qquad (2.19)$$

2.6   The particle in a spherical box

The particle in a cubic box has simple wave functions and energy eigenvalues. The problem of the particle in a spherical container is similar to the problem of the particle in a cubic box, and the matter waves form resonant, standing wave pattern inside the box, but there is considerable high mathematical complexity because of the spherical geometry.

2.6.1 Solving the Schrödinger equation

We assume that a particle of mass m moving in a spherical cell where the potential field, $V(r)$ is of the following form

$$V(r) = \begin{cases} 0 & \text{for } r < R_0 \\ \infty & \text{for } r \geq R_0 \end{cases}$$

where R_0 is the radius of the spherical cell.

The time-independent Schrödinger equation for this model is

$$\frac{\partial^2 \psi}{\partial x^2} + \frac{\partial^2 \psi}{\partial y^2} + \frac{\partial^2 \psi}{\partial z^2} + \frac{2m}{\hbar^2}(E - V(r))\psi = 0 \tag{2.20}$$

which

$$r = \sqrt{x^2 + y^2 + z^2} \tag{2.21}$$

The boundary conditions are

1. $\psi(r \leq R_0)$ remains finite

2. $\psi(R_0) = 0$

There is no way to break up Eqn. 2.20 into three ordinary differential equations involving the Cartesian coordinates, therefore, we use a spherical coordinate system. The relationship between these two systems is as follows

$$\begin{aligned} x &= r\sin\theta\cos\phi \\ y &= r\sin\theta\sin\phi \\ z &= r\cos\theta \end{aligned} \tag{2.22}$$

By substituting these conversion relations, Eqn. 2.20 becomes

$$\frac{1}{r^2}\frac{\partial}{\partial r}\left(r^2\frac{\partial \psi}{\partial r}\right) + \frac{1}{r^2\sin\theta}\frac{\partial}{\partial \theta}\left(\sin\theta\frac{\partial \psi}{\partial \theta}\right) + \frac{1}{r^2\sin^2\theta}\frac{\partial^2 \psi}{\partial \phi^2} + \frac{2m}{\hbar^2}(E - V(r))\psi = 0 \tag{2.23}$$

26

This equation is Helmholtz' equation, and we can write it in the following form

$$\frac{1}{r}\frac{\partial^2}{\partial r^2}(r\psi) + \frac{1}{r^2\sin\theta}\left(\frac{\partial}{\partial\theta}\left(\sin\theta\frac{\partial\psi}{\partial\theta}\right) + \frac{1}{\sin\theta}\frac{\partial^2\psi}{\partial\phi^2}\right) + k^2\psi = 0 \qquad (2.24)$$

where
$$k^2 = \frac{2m(E-V(r))}{\hbar^2} = \frac{2mE}{\hbar^2} \qquad (2.25)$$

We assume that the equation can be separated into two parts, one a function of r (radial part) and the other a function of θ and ϕ (angular part)

$$\psi = R(r)Y(\theta,\phi) \qquad (2.26)$$

If we substitute Eqn. 2.26 in Eqn. 2.24 and divide by $\psi = RY$, we find

$$\frac{1}{R}\frac{1}{r}\frac{\mathrm{d}^2}{\mathrm{d}r^2}(rR) + \frac{1}{r^2}\frac{1}{Y\sin\theta}\left(\frac{\partial}{\partial\theta}\left(\sin\theta\frac{\partial Y}{\partial\theta}\right) + \frac{1}{\sin\theta}\frac{\partial^2 Y}{\partial\phi^2}\right) + k^2 = 0 \quad (2.27)$$

and we have
$$\frac{1}{R}\frac{1}{r}\frac{\mathrm{d}^2}{\mathrm{d}r^2}(rR) + k^2 - \frac{\lambda}{r^2} = 0 \qquad (2.28)$$

where λ is a constant

$$\frac{1}{Y\sin\theta}\left(\frac{\partial}{\partial\theta}\left(\sin\theta\frac{\partial Y}{\partial\theta}\right) + \frac{1}{\sin\theta}\frac{\partial^2 Y}{\partial\phi^2}\right) = -\lambda \qquad (2.29)$$

If $k^2 \neq 0$, we change to the dimensionless radial coordinate $\rho = kr$, and obtain
$$\frac{\mathrm{d}^2 R}{\mathrm{d}\rho^2} + \frac{2}{\rho}\frac{\mathrm{d}R}{\mathrm{d}\rho} + \left(1 - \frac{\lambda}{\rho^2}\right)R = 0 \qquad (2.30)$$

The Bessel equation has the form

$$\frac{\mathrm{d}^2 R}{\mathrm{d}\rho^2} + \frac{1}{\rho}\frac{\mathrm{d}R}{\mathrm{d}\rho} + \left(1 - \frac{m^2}{\rho^2}\right)R = 0 \qquad (2.31)$$

It can be seen that Eqn. 2.30 is almost a Bessel equation.

2.6.2 Solving the Bessel equation

To convert Eqn. 2.30 to the Bessel equation, we make the substitution [3]

$$R = \frac{1}{\sqrt{\rho}} \, S \qquad (2.32)$$

After substituting this equation into Eqn. 2.30, we obtain

$$\frac{d^2 S}{d\rho^2} + \frac{1}{\rho}\frac{dS}{d\rho} + \left(1 - \frac{\lambda + 1/4}{\rho^2}\right) S = 0 \qquad (2.33)$$

this equation has the solution

$$S = A \, J_\beta(\rho) + B \, N_\beta(\rho) \qquad (2.34)$$

and

$$\beta = \sqrt{\lambda + 1/4} \qquad (2.35)$$

or

$$R = A \, \frac{1}{\sqrt{kr}} \, J_\beta(kr) + B \, \frac{1}{\sqrt{kr}} \, N_\beta(kr) \qquad (2.36)$$

which N is the Neumann function.

$$\psi = \left\{ A \, \frac{1}{\sqrt{kr}} \, J_\beta(kr) + B \, \frac{1}{\sqrt{kr}} \, N_\beta(kr) \right\} Y(\theta, \phi) \qquad (2.37)$$

The boundary condition that the angular function $Y(\theta, \phi)$ be everywhere single valued and finite leads to

$$\lambda = l(l + 1) \qquad (2.38)$$

$$Y = Y_l^m(\theta, \phi) \qquad (2.39)$$

then,

$$\beta = \sqrt{l^2 + l + 1/4} = l + 1/2 \qquad , l = 0, 1, 2, \ldots \qquad (2.40)$$

These Y_l^m are called spherical harmonics. The first few spherical harmonics are listed in [App. C].

Now we try to solve the ϕ dependent part of $Y(\theta, \phi)$

$$Y(\theta, \phi) = \Theta(\theta)\ \Phi(\phi) \tag{2.41}$$

The term Φ depends only on ϕ. This can be true only if this term is equal to a constant $(-m^2)$.

$$\frac{1}{\Phi}\frac{d^2\Phi}{d\phi^2} = -m^2 \tag{2.42}$$

therefore

$$\Phi(\phi) = A\ e^{im\phi} \tag{2.43}$$

As the boundary condition dictates that Φ should be single valued, m must be an integer in physical applications to insure that the eigenfunctions $\Phi_\alpha(\sin(\alpha\phi),\ \cos(\alpha\phi))$ be single valued, then

$$m = 0, \pm1, \pm2, \ldots \tag{2.44}$$

for each l , we have $2l + 1$ degenerate levels due to different values of m:
for $l = 0$, $m = 0$
for $l = 1$, $m = 0, \pm1$
for $l = 2$, $m = 0,\ \pm1,\ \pm2$
$\vdots$
After using the boundary conditions, we obtain

$$\psi = \left\{ A\ j_l(kr) + B\ n_l(kr) \right\} Y_l^m(\theta, \phi) \tag{2.45}$$

where spherical Bessel and Neumann functions are defined respectively by

$$j_l(x) = \sqrt{\frac{\pi}{2x}}\ J_{l+1/2}(x) \tag{2.46}$$

$$n_l(x) = \sqrt{\frac{\pi}{2x}}\ N_{l+1/2}(x). \tag{2.47}$$

These functions give the radial dependence of spherical waves. The spherical Bessel and Neumann functions can also be expressed in terms of sines

and cosines and inverse powers of x [3]. Here we expand the first term of Bessel function into series with respect to powers of x [App. A].

$$j_0(x) = \sqrt{\frac{\pi}{2x}} \; J_{1/2}(x) = \frac{\sqrt{\pi}}{2} \sum_{r=0}^{\infty} \frac{(-1)^r}{r! \, \Gamma(1/2 + r + 1)} \left(\frac{x}{2}\right)^{2r} \qquad (2.48)$$

Using the recursion relation of the Gamma function [App. B] , we find

$$\Gamma(1/2 + r + 1) = \frac{(2r+1)!}{2^{2r+1} r!} \sqrt{\pi} \qquad (2.49)$$

Substituting Eqn. 2.49 into Eqn. 2.48, we obtain

$$j_0(x) = \sum_{r=0}^{\infty} \frac{(-1)^r}{(2r+1)!} \, x^{2r} = \frac{\sin(x)}{x} \quad \text{(Taylor series for } \sin(x)) \qquad (2.50)$$

Using a recursion relation for the Bessel function and series solution we can find $j_l(x)$ as follows

$$j_l(x) = (-x)^l \left(\frac{1}{x}\frac{\mathrm{d}}{\mathrm{d}x}\right)^l \left(\frac{\sin(x)}{x}\right) \qquad (2.51)$$

$n_l(x)$ can be calculated by the same way

$$n_l(x) = -(-x)^l \left(\frac{1}{x}\frac{\mathrm{d}}{\mathrm{d}x}\right)^l \left(\frac{\cos(x)}{x}\right) \qquad (2.52)$$

We can easily calculate $j_l(x)$ Fig. 2.2 and $n_l(x)$ for small l

$$\begin{aligned}
j_0(x) &= \frac{\sin(x)}{x} \\
j_1(x) &= \frac{\sin(x)}{x^2} - \frac{\cos(x)}{x} \qquad (2.53) \\
j_2(x) &= \left(\frac{3}{x^3} - \frac{1}{x}\right) \sin(x) \\
&\;\;\vdots \qquad\qquad\qquad\qquad\qquad\qquad (2.54)
\end{aligned}$$

30

and

$$
\begin{aligned}
n_0(x) &= \frac{\cos(x)}{x} \\
n_1(x) &= -\frac{\sin(x)}{x} - \frac{\cos(x)}{x^2} \\
n_2(x) &= -\frac{3}{x^2}\sin(x) - \left(\frac{3}{x^3} - \frac{1}{x}\right)\cos(x)
\end{aligned}
\tag{2.55}
$$

$$
\vdots
\tag{2.56}
$$

The spherical Neumann function is rejected because it diverges at the origin $(x = 0)$, therefore we have

$$
R = A\, j_l\left(\frac{\sqrt{2mE}}{\hbar}\, r\right)
\tag{2.57}
$$
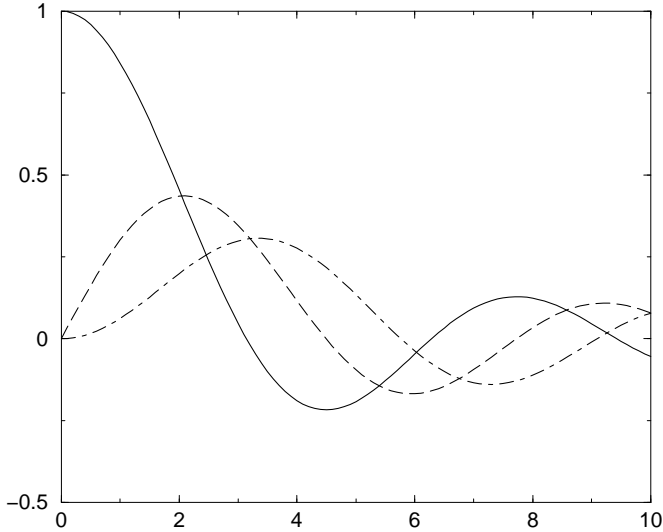
Figure 2.2: Bessel j functions.

To satisfy the boundary condition $\psi(R_0) = 0$ for all angles, we require

$$
\frac{\sqrt{2mE_{l,n}}}{\hbar} R_0 = j_{l,n}^*
\tag{2.58}
$$

31

and

$$E_{l,n} = \frac{\hbar^2 (k_{l,n} R_0)^2}{2mR_0^2} = \frac{\hbar^2 (j_{l,n}^*)^2}{2mR_0^2} \qquad (2.59)$$

or

$$k_{l,n} R_0 = j_{l,n}^* \qquad (2.60)$$

where $j_{l,n}^*$ denotes the roots of the j_l that $j_l(j_{l,n}^*) = 0$, and the n index shows the nth zero of j_l. The inclusion of this boundary condition quantizes the energy E. The smallest $j_{l,n}^*$ is the first zero of j_0

$$j_0(x) = \frac{\sin(x)}{x} \qquad \text{for} \quad j_{0,1}^* = \pi \qquad (2.61)$$

$$E_{\min} = \frac{\pi^2 \hbar^2}{2mR_0^2} = \frac{h^2}{8mR_0^2} \qquad (2.62)$$

for $l = 0$

$$E_{\min} = \frac{n^2 h^2}{8mR_0^2} \qquad (2.63)$$

asymptotic behaviour of the j_l for $x \to \infty$ is

$$\lim_{x \to \infty} j_l(x) = \frac{1}{x} \cos\left(x - (l+1)\,\pi/2\right) \qquad (2.64)$$

The functions $j_l(x)$ have an infinite number of real zeros. The first zeros for different ls are obtained from [5]

$$\begin{aligned} j_{l,1}^* \quad &\simeq (l+1/2) + 1.85575(l+1/2)^{1/3} + 1.03315(l+1/2)^{-1/3} \\ &\quad -0.00397(l+1/2)^{-1} - 0.0908(l+1/2)^{-5/3} + \ldots \end{aligned} \qquad (2.65)$$

where $v = (l+1/2)$.

Chapter 3

Statistical Thermodynamics

3.1   Introduction

In the previous section we showed how the quantum states or microstates can be calculated from quantum mechanics rules. However, quantum mechanics cannot supply the macroscopic properties such pressure, heat capacity, viscosity, entropy, Helmholtz free energy etc. A realistic view of a macroscopic system is that the system makes a very rapid random transitions among its quantum states. A macroscopic measurement senses only an average of the properties of the quantum states. Statistical mechanics shows the way of averaging among the quantum states.

3.2   The microcanonical ensemble

We focus first on a closed system of given volume, given energy and given number of particles. The parameters U, V, and N are the only constraints of the system. The external constraints imposed on the system specify the permissible quantum states. As the transitions between quantum states are due to the random processes, it is reasonable to suppose that a macroscopic system samples every permissible quantum state with equal probability.

The assumption of equal probability of all permissible microstates is the fundamental postulate of statistical mechanics. If some external constraint is removed, the number of permissible microstates increases. Transitions occur to these newly available states and the number of microstates increases to the maximum permitted by the imposed constraints.

The entropy also increases to the maximum permitted by the imposed constraints. Therefore the entropy can be derived from the number of microstates consistent with the imposed macroscopic constraints [9]. Since the entropy is additive (extensive) but the number of microstates is multiplicative we must identify the entropy with the logarithm of the number of available microstates.Thus

$$S = k_{\mathrm{B}} \ln \Omega \tag{3.1}$$

where S is the entropy, Ω is the number of microstates and k_{B} is Boltzmann's constant; it is chosen in agreement with the Kelvin scale of tem-

perature $1/T = \partial S/\partial U$ where U is the internal energy of the system. Calculating the logarithm of the number of states available to the system we can obtain S as a function of the constraints the internal energy volume and the amount of substance of the system. This is the *microcanonical formalism.* of statistical mechanics. From the other point of view, we can consider an ensemble which is composed of members with the same values of N , V, and U. The microcanonical ensemble is a collection of these members (replicas) of the actual system Fig. 3.1 .

At instant t, the members are distributed over the Ω possible quantum states. Each member fluctuates among the possible states independently.

(N, V, E) fixed

ψ_i

Isolated from surroundings
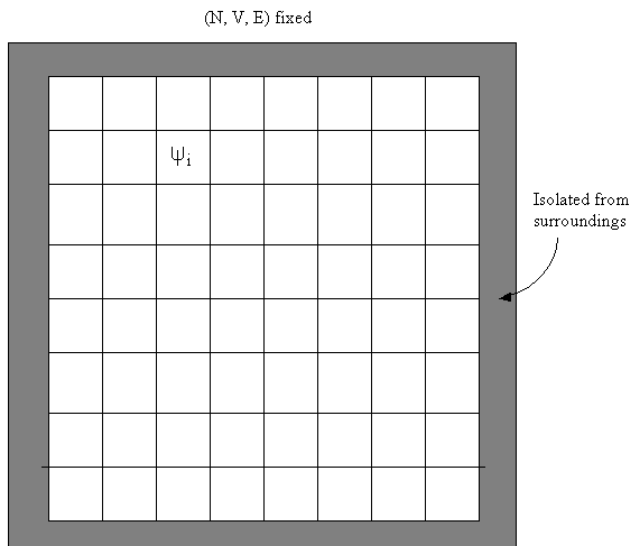
Figure 3.1: The microcanonical ensemble.

For other constraints there are other kinds of ensembles. Some examples are:

1. The canonical ensemble with (N, V, T) fixed .

2. The grand canonical ensemble with (μ, V, T) fixed where μ is chemical potential.

3. The isobaric–isothermal ensemble with (N, p, T) fixed .

3.3   The canonical ensemble

The microcanonical formalism is only useful for a few highly idealized models. We remove the limitation of energy value to consider a system in contact with a thermal reservoir (rather than an isolated system). The statistical mechanics of a system in contact with a thermal reservoir is called "canonical formalism". All energy values are available to the system. In contrast to the microcanonical formalism each state does not have the same probability. The problem in the canonical formalism is the determination of the probability distribution of the system among its microstates. The system plus the reservoir constitute a closed system, therefore the principle of equal probability applies. A thermal reservoir is defined as a reversible heat source. It is so large that any heat transfer does not change the temperature of the reservoir. It can be shown [9] that the probability of a subsystem being in state j is f_j.

$$f_j = \frac{\Omega_{\text{res}}(E_{\text{tot}} - E_j)}{\Omega_{\text{tot}}(E_{\text{tot}})} \tag{3.2}$$

Here E_{tot} and Ω_{tot} are the total energy and the total number of states of the system plus reservior, respectively. The quantity $\Omega_{\text{tot}}(E_{\text{tot}} - E_j)$ is the number of states available to the reservoir when the subsystem is in the jth state. Using Eqn. 3.1 we obtain

$$f_j = \frac{\exp\left(k_{\text{B}}^{-1} S_{\text{res}}(E_{\text{tot}} - E_j)\right)}{\exp\left(k_{\text{B}}^{-1} S_{\text{tot}}(E_{\text{tot}})\right)} \tag{3.3}$$

Using additivity of entropy the denominator can be shown as

$$S_{\text{tot}}(E_{\text{tot}}) = S(U) + S_{\text{res}}(E_{\text{tot}} - U) \tag{3.4}$$

36

where U is the average value of the energy of subsystem. If we expand $S_{\text{res}}(E_{\text{tot}} - E_j)$ around the equilibrium point $(E_{\text{tot}} - U)$ we obtain

$$
\begin{aligned}
S_{\text{res}}(E_{\text{tot}} - E_j) &= S_{\text{res}}(E_{\text{tot}} - U + U - E_j) \\
&= S_{\text{res}}(E_{\text{tot}} - U) + (U - E_j)/T
\end{aligned}
\tag{3.5}
$$

The upper order terms in the expansion are zero (because of the definition of a reservoir). Applying Eqns. 3.4 and 3.5 into Eqn. 3.3 we obtain

$$
f_j = e^{(1/k_{\text{B}}T)(U - TS(U))} e^{-(1/k_{\text{B}}T)E_j}
\tag{3.6}
$$

$(U - TS(U))$ is the Helmholtz energy of the system. We let

$$
\beta = \frac{1}{k_{\text{B}}T}
\tag{3.7}
$$

to obtain the fundamental result for the probability f_j of the subsystem being in the state j.

$$
f_j = e^{\beta A} e^{-\beta E_j}
\tag{3.8}
$$

The $e^{\beta A}$ plays the role of a state-independent normalization factor in Eqn. 3.8

$$
\sum_j f_j = e^{\beta A} \sum_j e^{-\beta E_j} = 1
\tag{3.9}
$$

or

$$
e^{-\beta A} = Q
\tag{3.10}
$$

where Q is the "canonical partition function" and is defined as

$$
Q = \sum_j e^{-\beta E_j}
\tag{3.11}
$$

Given a list of all states j of the system, and their energies E_j, we can calculate the partition function. The partition function is a function of temperature (or β) and the parameters $(V, N_1, N_2, \ldots)$ that determine the energy levels. Finally the Helmholtz energy of the system can be obtained by

$$
A = -k_{\text{B}}T \ln Q
\tag{3.12}
$$

The probability of occupation of the jth state can be written as

$$
\frac{e^{-\beta E_j}}{\sum_i e^{-\beta E_i}}
\tag{3.13}
$$

3.4 Thermodynamic properties

The ensemble average of any dynamical property of system can be obtained using Eqn. 3.13. A dynamical property is a property whose value is determined by the quantum states of the system, f_j, or classically a property which is defined as a function of the phase space coordinates and time. Examples are pressure and energy.

The average energy is then expected to be

$$U = \sum_j E_j f_j = \frac{\sum_j E_j \mathrm{e}^{-\beta E_j}}{\sum_i \mathrm{e}^{-\beta E_i}} \tag{3.14}$$

or

$$U = -\left(\frac{\partial \ln Q}{\partial \beta}\right)_{N,V} \tag{3.15}$$

The observed pressure of the system is

$$p = \sum_j p_j f_j \tag{3.16}$$

The pressure in the state j is

$$p_j = -\left(\frac{\partial E_j}{\partial V}\right)_N \tag{3.17}$$

therefore

$$p = \frac{1}{\beta}\left(\frac{\partial \ln Q}{\partial V}\right)_{N,\beta} \tag{3.18}$$

Equation 3.18 is the equation of state in statistical mechanics. The thermodynamic properties [8] in terms of the canonical partition function are summarized in table 3.1.

3.5 Factorization of canonical partition function

We consider a system composed of N distinguishable "elements". An element is a noninteracting excitation mode of the system. For an ideal gas

the "elements" refer to the excitations of the individual molecules while for a strongly interacting systems the elements may be vibrational modes or electromagnetic modes. The energy of the system is a sum over the energies of the elements which are independent and noninteracting. The energy of the ith element in its jth state is ϵ_{ij}. Then the canonical partition function is

$$
\begin{aligned}
Q &= \sum_{j,j',j'',\dots} \mathrm{e}^{-\beta(\epsilon_{1j}+\epsilon_{2j'}+\epsilon_{3j''}+\dots)} \\
&= \sum_{j,j',j'',\dots} \mathrm{e}^{-\beta\epsilon_{1j}}\,\mathrm{e}^{-\beta\epsilon_{2j'}}\,\mathrm{e}^{-\beta\epsilon_{3j''}}\,\dots \\
&= \sum_{j} \mathrm{e}^{-\beta\epsilon_{1j}} \sum_{j'} \mathrm{e}^{-\beta\epsilon_{2j'}} \sum_{j''} \mathrm{e}^{-\beta\epsilon_{3j''}}\,\dots \\
&= q_1\,q_2\,q_3\dots
\end{aligned}
\tag{3.19}
$$

where the q_i is the partition function of the ith element

$$
q_i = \sum_{j} \mathrm{e}^{-\beta\epsilon_{ij}}
\tag{3.20}
$$

Furthermore the Helmholtz energy is additive over elements

$$
-\beta A = \ln Q = \ln q_1 + \ln q_2 + \dots
\tag{3.21}
$$

The molecules of a gas have different excitation modes, three translational modes, vibrational modes, rotational modes, electronic modes, and modes of excitation of the nucleus. It is assumed that these modes are independent then the partition function is as follows

$$
Q = Q_{\text{trans}}\,Q_{\text{vib}}\,Q_{\text{rot}}\,Q_{\text{elect}}\,Q_{\text{nucl}}
\tag{3.22}
$$

Another assumption is that the Hamiltonian operator can be separated into two independent parts. One involving the center of mass modes (translational modes) and the other involving the intramolecular modes (vibration, rotation, etc.). This yields two independent sets of quantum

states, one for translation and the other for internal modes, respectively. Then the canonical partition function can be separated into two parts

$$Q = Q_{\text{trans}}(N, V, T) \; Q_{\text{int}}(N, T) \tag{3.23}$$

The Q_{int} part is independent of volume because it contains the intramolecular degrees of freedom. This assumption requires that Q_{int} has the same value for a dense fluid or an ideal gas. This assumption is exact in the ideal gas limit. It also holds for monoatomic fluids for all densities, because electronic energy is the only intramolecular interaction. For normal liquid densities (up to the triple point) the effect of density on the electronic wave function is negligible [8]. Polyatomic molecules have rotational and vibrational modes. At high densities particularly in the liquid state these internal modes may be affected by density. However, it is common to assume that Q_{int} is independent of density.

3.6 Translational partition function for an ideal gas

We apply the general results of the previous sections to an ideal gas. An ideal gas is a gas dilute enough that intermolecular interactions can be neglected (unless such interactions make no contribution to the energy, like collisions of hard mass points). A monatomic ideal gas has translation, electronic and nucleur degrees of freedom and the electronic and nucleur Hamiltonians are separable. To evaluate the translational partition function, we can use energy eigenvalues of the particle in a cubic box Eqn. 2.19.

$$
\begin{aligned}
q_{\text{trans}} &= \sum_{n_x, n_x, n_x = 1}^{\infty} \mathrm{e}^{-\beta \epsilon_{n_x, n_y, n_z}} \\
&= \sum_{n_x=1}^{\infty} \exp\left(-\frac{\beta h^2 n_x^2}{8 m R_0^2}\right) \sum_{n_y=1}^{\infty} \exp\left(-\frac{\beta h^2 n_y^2}{8 m R_0^2}\right) \sum_{n_z=1}^{\infty} \exp\left(-\frac{\beta h^2 n_z^2}{8 m R_0^2}\right) \\
&= \left(\sum_{n_x=1}^{\infty} \exp -\frac{\beta h^2 n_x^2}{8 m R_0^2}\right)^3 \tag{3.24}
\end{aligned}
$$

At high temperature limit, n_x, n_y, and n_z are very large ($O(10^{10})$), when the dimensions of container is of the order of (10 cm), it can be shown that the terms of the summations differ very little from each other and we can assume the terms vary continuously. The difference between the arguments of the exponential in going from n_x to $n_x + 1$ is called Δ and is given by

$$\Delta = \frac{\beta h^2 (n_x + 1)^2}{8mR_0^2} - \frac{\beta h^2 n_x^2}{8mR_0^2} = \frac{\beta h^2 (2n_x + 1)}{8mR_0^2} \qquad (3.25)$$

At room temperature, for $m = 10^{-22}$ g and $a = 10$ cm this difference is

$$\Delta \approx (2n_x + 1) \times 10^{-20} \qquad (3.26)$$

Thus the summation in Eqn. 3.24 may be replaced by an integral.

$$q_{\text{trans}}(V, T) = \left(\int_0^\infty e^{-\beta h^2 n^2 / 8mR_0^2} \mathrm{d}n \right)^3 = \left(\frac{2\pi mkT}{h^2} \right)^{3/2} V \qquad (3.27)$$

where $V = R_0^3$.

The factor $(h^2 / 2\pi mkT)^{1/2}$ has a dimension of length and is denoted by Λ. Then

$$q_{\text{trans}} = \frac{V}{\Lambda^3} \qquad (3.28)$$

The kinetic energy of an ideal gas can be calculated by

$$\bar{\epsilon}_{\text{trans}} = kT^2 \left(\frac{\partial \ln q_{\text{trans}}}{\partial T} \right) \qquad (3.29)$$

and

$$\bar{\epsilon}_{\text{trans}} = \frac{3}{2} kT \qquad (3.30)$$

Since $\epsilon_{\text{trans}} = p^2 / 2m$, the average momentum is $(mkT)^{1/2}$ thus Λ is h/p, which is defined in Sec. 2.2 as de Broglie wavelength of the particle. The classical statistics is valid only if $\Lambda^3 / V \ll 1$. It means that the thermal de Broglie wavelength must be small compared to the dimensions of the container or quantum effects decrease as de Broglie wavelength becomes small.

To calculate the canonical partition function, if we evaluate Q as q^N, and then calculate the Helmholtz energy A, we obtain a non–extensive Helmholtz energy. To identify Q as q^N it it is assumed that the particles are distinguishable, like a set of billiard balls. In quantum mechanics non-localized particles of one species are indistinguishable (Sec. 2.4). It means the particle are identical and that their wave functions must be antisymmetric or symmetric on interchanging any two of the particles. This behavior has no classical analogue. Now we need only a classical solution. It has done by recognizing q^N is the partition function of a set of distinguishable particles. By division by $N!$ which is all permutations of the "labels" among the N distinguishable particles, we can obtain the partition function for indistinguishable particles.

$$Q = \left(\frac{1}{N!}\right) q_{\text{trans}}^N \tag{3.31}$$

At very low temperature some errors can occur when division by $N!$ is done to count the states. We consider a model system of two identical particles, each of which can exist in one of two states (Fig. 3.2).

There are four probable ways for classical particles which are distinguishable. It can be divided by 2! to obtain the number of ways for indistinguishable particles. If the particles are fermions, only one particle is permitted to occupy a state, therefore, there is only one permissible way for the system. For bosons, of which any number of particles are permitted to occupy an orbital state, there are three different ways for the system. At sufficiently high temperature where many orbitals are available for the particles of a gas, the probability of two particles being in the same orbital is very small. For temperatures above about 20 K assumption of dividing by $N!$ is valid. When temperature is much lower than this, it is necessary to consider the probability of several particles being in one orbital state and Bose–Einstein or Fermi–Dirac statistics must be used. Application of quantum statistics is necessary to study of electrons, photons, and liquid helium [7].

Using the assumption in Sec. 3.6 that the partition function can be separated into a translational part and an internal part, and using Eqn.
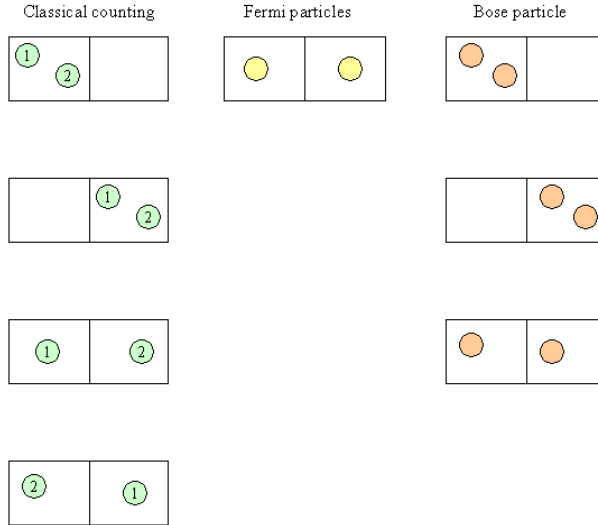
Figure 3.2: Comparison of the probable ways for distribution of two classical particles, fermions, and bosones .

3.31 we obtain

$$Q = \frac{\left(q_{\text{trans}} q_{\text{int}}\right)^N}{N!} \tag{3.32}$$

q_{trans} is the only part that contributes to pressure. Substituting Eqns. 3.27 and 3.31 into the equations of Table 3.1 gives the translational contribution to the thermodynamic properties Table (3.2).

Table 3.1: Thermodynamic properties in terms of
the canonical partition function.

partition function	$Q = \sum_j \exp\left(\frac{-E_j}{k_B T}\right)$
internal energy	$U = k_B T^2 \left(\frac{\partial \ln Q}{\partial T}\right)_{N,V}$
pressure	$p = k_B T \left(\frac{\partial \ln Q}{\partial V}\right)_{N,T}$
enthalpy	$H = k_B T^2 \left(\frac{\partial \ln Q}{\partial T}\right)_{N,V} + k_B TV \left(\frac{\partial \ln Q}{\partial V}\right)_{N,T}$
heat capacity in constant V	$C_V = \left(\frac{\partial U}{\partial T}\right)_{N,V}$
heat capacity in constant p	$C_p = \left(\frac{\partial H}{\partial T}\right)_{N,p}$
entropy	$S = k_B \ln Q + \left(\frac{U}{T}\right)$
Helmholtz free energy	$A = -k_B T \ln Q$
Gibbs free energy	$G = -k_B T \ln Q + k_B TV \left(\frac{\partial \ln Q}{\partial V}\right)_{N,T}$
chemical potential	$\mu = -k_B T \left(\frac{\partial \ln Q}{\partial N_\alpha}\right)_{T,V,N_{\beta \neq \alpha}}$

Table 3.2: Translational contribution to thermodynamic properties .

internal energy	$U_{\text{trans}} = \frac{3}{2}Nk_{\text{B}}T$
pressure	$p = p_{\text{trans}} = \frac{Nk_{\text{B}}T}{V}$
enthalpy	$H_{\text{trans}} = \frac{5}{2}Nk_{\text{B}}T$
heat capacity in constant V	$C_{V,\text{trans}} = \frac{3}{2}Nk_{\text{B}}$
heat capacity in constant p	$C_{p,\text{trans}} = \frac{5}{2}Nk_{\text{B}}$
entropy	$S_{\text{trans}} = Nk_{\text{B}}\ln\left(\Lambda^{-3}\frac{V}{N}\right) + \frac{5}{2}Nk_{\text{B}}$
Helmholtz free energy	$A_{\text{trans}} = -Nk_{\text{B}}T\ln\left(\Lambda^{-3}\frac{V}{N}\right) - Nk_{\text{B}}T$
Gibbs free energy	$G_{\text{trans}} = -Nk_{\text{B}}T\ln\left(\Lambda^{-3}\frac{V}{N}\right)$
chemical potential	$\mu_{\text{trans}} = -k_{\text{B}}T\ln\left(\Lambda^{-3}\frac{V}{N}\right)$

Chapter 4

Equations of State

4.1 The van der Waals Equation of State

The equation of state for a ideal gas, $pV = NRT$ is only valid when a gas is highly dilute, but even at atmospheric pressure this ideal gas law has appreciable deviations.

The van der Waals equation of state was the first equation which can predict both vapor and liquid phases. According to van der Waals' assumptions the actual volume available for molecules in a container with volume V is $(V - b)$ where b is called covolume and denotes the finite diameter of a molecule. On the other hand, intermolecular attraction decreases the pressure. He assumed that the attraction part is proportional to the number of molecules in a volume unit and inversely proportional to volume. The correction proposed by van der Waals for intermolecular attractions was $-a/V_\mathrm{m}^2$. It can be assumed that the corrected volume and corrected pressure should obey the ideal gas law

$$\left(p + \frac{a}{V_\mathrm{m}^2}\right)(V_\mathrm{m} - b) = RT \tag{4.1}$$

where T is temperature, p is pressure V_m is molar volume and R is the gas constant. This equation can be written as an equation for pressure which contains two terms correspond to repulsive and attractive contributions to pressure:

$$p = \frac{RT}{(V_\mathrm{m} - b)} - \frac{a}{V_\mathrm{m}^2} \tag{4.2}$$

Separating the repulsive and attractive terms in equation of states is quite valuable for the representation of fluid properties. The a and b parameters in the van der Waals equation can be obtained from the critical properties of the fluid. The critical point conditions are

$$\frac{\partial p}{\partial V_\mathrm{m}} = \frac{\partial^2 p}{\partial V_\mathrm{m}^2} = 0 \tag{4.3}$$

The values of a and b at the critical point can be calculated by

$$a_c = \frac{27}{64} \frac{R^2 T_c^2}{p_c^2} \tag{4.4}$$

$$b_c = \frac{1}{8}\frac{RT_c}{p_c} \qquad (4.5)$$

On the other hand the van der Waals equation can be rewritten as a cubic polynomial with respect to volume. Therefore, it can be solved analytically for the volume e.g. by means of Cardono's formulas. The most important features of the van der Waals equation are:

1. The constants a and b are valid for both gas and liquid phases.

2. The equation can predict the vapor–liquid critical point

However, the van der Waals equation of state is only a crude approximation. It can not predict the pVT data of fluid phases accurately.

4.2   Van der Waals type equations

Many researchers tried to improve the van der Waals equation. In 1881, Clausius [29] replaced the volume in van der Waals attractive term by $(V_\mathrm{m} + c)$.

$$p = \frac{RT}{(V_\mathrm{m} - b)} - \frac{a}{(V_\mathrm{m} + c)^2} \qquad (4.6)$$

In 1899, Berthelot [30] assumed a temperature dependent attractive parameter $a_T = a/T$.

The techniques used in the improvement of the van der Waals type equation concentrated in two areas:

1. Modification of the $p(V_\mathrm{m})$ functional form to improvement the prediction of volumetric properties

2. Introducing a temperature dependent attractive parameter to control the vapor pressure predictions.

Examples of the first category are the equations of Redlich–Kwong (RK) [10] , Peng–Robinson (PR), [12], Schmidt–Wenzel (SW) [15] , Clausius (C) [29]. The Soave form of the Redlich–Kwong equation (SRK) [11], and Stryjek–Vera (SV) [21] are examples of the second category.

4.2.1 Attractive Term

It is adequate to use an extended form of the van der Waals equation of state. One of these extended forms which can be used for the currently popular cubic equation is [32]:

$$p = \frac{RT}{(V_{\mathrm{m}} - b)} - \frac{a}{(V_{\mathrm{m}}^2 + ubV_{\mathrm{m}} + wb^2)} \tag{4.7}$$

The denominator of the second term in Eqn. 4.7 is a quadratic expression in volume, $(V_{\mathrm{m}}^2 + ubV_{\mathrm{m}} + wb^2)$ which replaces the V_{m}^2 term in the attractive term of the van der Waals Eqn. 4.2. When $u = w = 0$, Eqn. 4.7 can be reduced to the Eqn. 4.2. In Redlich–Kwong (RK) equation $u = 1$ and $w = 0$, and in its various forms, the Peng–Robinson (PR) equation $u = 2$ and $w = -1$, the Heyen equation [14] $u + w = 1$, the Schmidt–Wenzel (SW) [15] $u + w = 1$, etc.

The most general form for a cubic equation of state has the form [35].

$$p = \frac{RT}{(V_{\mathrm{m}} - b)} - \frac{a(V_{\mathrm{m}} - \eta)}{(V_{\mathrm{m}} - b)(V_{\mathrm{m}}^2 + \delta V_{\mathrm{m}} + \epsilon)} \tag{4.8}$$

This equation has five adjustable parameters b, a, η, δ and ϵ which can be temperature dependent [34] .

The temperature dependence of the a parameter plays an important role in calculating the vapor pressure. Wilson [36] was first one who introduced a general form for temperature dependence of a parameters.

$$a = a_c \alpha \tag{4.9}$$

where a_c is the value of a at the critical point and α is

$$\alpha = T_{\mathrm{R}}[1 + (1.57 + 1.62\omega)(T_{\mathrm{R}}^{-1})] \tag{4.10}$$

where $T_{\mathrm{R}} = T/T_{\mathrm{c}}$ is the reduced temperature and ω is the acentric factor and represents the geometric shape of the molecule. For monatomic gases ω is almost equal to zero. It increases with the size and polarity of a molecule [34]. The values of acentric factor are tabulated in various sources

([37, 38, 39, 40]). Soave proposed a simple and accurate expression for the temperature dependence of α:

$$\alpha = [1 + mT_{\mathrm{R}}^{1/2}]^2 \tag{4.11}$$

where m is a quadratic function of the acentric factor. Many investigators used the Soave's function (Peng and Robinson Schmidt and Wenzel, Patel and Teja [18], Adachi et al. [19, 20] Watson et al. [41] and others). They changed only the $m(\omega)$ function to put it into their own equations of state.

Some of the modifications of the attractive term of the van der Waals equation are tabulated in 4.1.

4.2.2 Repulsive Term

The other way to modify the van der Waals equation of state is adjusting the repulsive term. Adachi et al. [19] evaluated 16 three–parameter equations of states for the representation of saturation properties and the high density region. The repulsive terms proposed by Scott [27], Guggenheim [25], Carnahan–Starling [26] were combined with the attractive parts of Redlich–Kwong, Clausius, Peng–Robinson and Harmens–Knapp to obtain the expression for the equations.

The cubic equations of states need at least three adjustable parameters which at least one of them should be temperature dependent [34].

Some of the modifications of the repulsive term of the van der Waals equation are tabulated in 4.3.

4.3 Generalized van der Waals–type equation of state

Many researchers tried to show the contributions of the repulsion and attraction forces to thermodynamic properties of fluids. It can be theoretically shown ([42, 43, 44]) that the pressure equation can be separated into two parts, the repulsive and attractive terms for some model intermolecular potentials. The repulsive part of van der waals equation is very crude

Table 4.1: Modifications to the attractive parts of the van der Waals Equation
.

Equation	Attractive Term (p_{att})
Redlich–Kwong (RK)(1949) [10]	$\frac{a}{T^{0.5}V_{\mathrm{m}}(V_{\mathrm{m}}+b)}$
Soave (SRK)(1972) [11]	$\frac{a(T)}{V_{\mathrm{m}}(V_{\mathrm{m}}+b)}$
Peng–Robinson (PR)(1976) [12]	$\frac{a(T)}{[V_{\mathrm{m}}(V_{\mathrm{m}}+b)+b(V_{\mathrm{m}}-b)]}$
Fuller (1976) [13]	$\frac{a(T)}{V_{\mathrm{m}}(V_{\mathrm{m}}+cb)}$
Heyen(1980)(Sandler,1994) [14]	$\frac{a(T)}{[V_{\mathrm{m}}^2+(b(T)+c)V_{\mathrm{m}}-b(T)c]}$
Schmidt–Wenzel (SW)(1980) [15]	$\frac{a(T)}{(V_{\mathrm{m}}^2+ubV_{\mathrm{m}}+wb^2)}$
Harmens–Knapp (1980) [16]	$\frac{a(T)}{(V_{\mathrm{m}}^2+V_{\mathrm{m}}cb-(c-1)b^2)}$
Kubic (1982) [17]	$\frac{a(T)}{(V_{\mathrm{m}}+c)^2}$
Patel–Teja (PT)(1982) [18]	$\frac{a(T)}{[V_{\mathrm{m}}(V_{\mathrm{m}}+b)+c(V_{\mathrm{m}}-b)]}$
Adachi et al. (1983) [19]	$\frac{a(T)}{(V_{\mathrm{m}}-b_2)(V_{\mathrm{m}}+b_3)}$
Stryjek–Vera (SV)(1986a) [21]	$\frac{a(T)}{(V_{\mathrm{m}}^2+2bV_{\mathrm{m}}-b^2)}$
Yu–Lu (1987) [22]	$\frac{a(T)}{V_{\mathrm{m}}(V_{\mathrm{m}}+c)+b(3V_{\mathrm{m}}+c)}$
Trebble–Bishnoi (TB)(1987) [23] 52	$\frac{a(T)}{V_{\mathrm{m}}^2+(b+c)V_{\mathrm{m}}-(bc+d^2)}$
Schwartzentruber–Renon (1989) [24]	$\frac{a(T)}{(V_{\mathrm{m}}+c)(V_{\mathrm{m}}+2c+b)}$

Table 4.2: Comparison of saturated vapor pressures and liquid and vapor volumes using some cubic EOS. [34] , $\delta(x) = (100/N) \sum | x_i^{cal} - x_i^{exp} | /x_i^{exp}$.

Model	$\delta(p_{sat})$	$\delta(V_{liq})$	$\delta(V_{vap})$
Soave	1.5	17.2	3.1
Peng–Robinson	1.3	8.2	2.7
Fuller	1.3	2.0	2.8
Schmidt–Wenzel	1.0	7.9	2.6
Harmens–Knapp	1.5	6.6	3.0
Heyen	5.0	1.9	7.2
Patel–Teja	1.3	7.5	2.6
Kubic	3.5	7.4	15.9
Adachi	1.1	7.4	2.5
Trebble and Bishnoi	2.0	3.0	3.1
Yu–Lu	1.3	3.3	2.2

estimation, therefore, better expressions have been proposed to be used as reference terms in equations of state. Carnahan and Starling proposed an expression for the nonspherical hard convex bodies, Boublík and Nezbeda a more general form of this expression.

Deiters [50, 51] developed a generalized van der Waals equation of state. This equation is a semiempirical equation of state which has been developed for non–polar and weakly polar fluids. The square well model is used as the intermolecular pair potential. The equation involves corrections for nonspherical molecules, soft repulsion potential, and three–body effects. This equation of state covers the total fluid range with good accuracy and has only three adjustable parameters determined from T_c, p_c, and v_c. The compressibility factor varies between 0.29 and 0.21, therefore it covers the experimentally observed range (for nonpolar and moderately

Table 4.3: Modifications to the repulsion parts of the van der Waals Equation.[1]$\xi = 0.74048 V_{\mathrm{m}}^0/V_{\mathrm{m}}$, V_{m}^0 is the close–packed volume, and α is a nonsphericity parameter .

Equation	Repulsive Term (p_{rep})
Guggenheim (1965) [25]	$\dfrac{RT}{V_{\mathrm{m}}(V_{\mathrm{m}}-b)^4}$
Carnahan–Starling (1969) [26]	$\dfrac{RT(V_{\mathrm{m}}^3+bV_{\mathrm{m}}^2+b^2V_{\mathrm{m}}-b^3)}{V_{\mathrm{m}}(V_{\mathrm{m}}-b)^3}$
Scott et al. (1971) [27]	$\dfrac{RT(V_{\mathrm{m}}+b)}{V_{\mathrm{m}}(V_{\mathrm{m}}-b)}$
Boublík–Nezbeda[1](1981) [28]	$\dfrac{RT(1+(3\alpha-2)\xi+(3\alpha^2-3\alpha+1)\xi^2-\alpha^2\xi^3)}{V_{\mathrm{m}}(1-\xi)^3}$

polar substances). It has the form:

$$p = \frac{RT}{b}\rho\left[1 + cc_0\frac{4\xi - 2\xi^2}{(1-\xi)^3}\right] - \frac{Ra}{b}\rho^2\frac{\tilde{T} + \lambda\rho}{Y}\left[\exp(\frac{Y}{\tilde{T} + \lambda\rho}) - 1\right]I_1 \quad (4.12)$$

with

$$\rho = \frac{b}{V_m} \quad , \quad \xi = \frac{\pi\sqrt{2}}{6}\rho \quad , \quad \tilde{T} = \frac{cT}{a} \quad , \quad c_0 = 0.06887$$

$$y = f^2 - c^{-5.5}f(1-f) + \left(1 - \frac{0.65}{c}\right)(1-f)^2 \quad (4.14)$$

$$f = \exp\left(cc_0\frac{3\xi^2 - 4\xi}{(1-\xi)^2}\right) \quad (4.15)$$

$$\lambda = -0.06911c \quad , \quad \gamma = 1 - 0.0697816(c-1)^2$$

$$I_1(\rho) = \frac{\gamma^2}{c^2}\sum_0^5 h_i(i+1)\gamma^i\rho^i. \quad (4.17)$$

The h_i are listed in Table 4.4.

The three adjustable parameters are: the potential well depth a, the covolume b, and the number of additional degrees of freedom c.

4.4 Mixtures

Equations of state can be used for mixtures if we have a satisfactory way to obtain their parameters for mixtures. Using mixing and combining rules we can calculate the properties of mixture from the properties of pure components.

Table 4.4: Polynomial coefficients of $I_1(\rho)$.

i	h_i
0	7.0794046
1	12.08351455
2	-53.6059
3	143.6681
4	-181.1554682
5	78.5739255

4.4.1 Mixing rules

The most widely used method to extend equation of state to nonpolar mixtures is the "classical one fluid" method proposed by van der Waals in 1980. He assumed that the properties of a mixture are averages of the properties of the pure components. The simplest function for the attractive parameter is

$$a = \sum \sum x_i x_j a_{ij} \tag{4.18}$$

where the cross term a_{ij} is related to the pure terms a_{ii} and a_{jj} by

$$a_{ij} = (a_{ii} a_{jj})^{1/2} (1 - k_{ij}) \tag{4.19}$$

k_{ij} is an adjustable parameter. the covolume b is usually expressed by a linear mixing rule

$$b = \sum x_i b_i \tag{4.20}$$

However many authors use a quadratic form for b.

$$a_{ij} = (a_{ii} a_{jj})^{1/2} (1 - k_{ij}) \tag{4.21}$$

The classical quadratic mixing rules are adequate for nonpolar and weakly polar components. Adachi and Sugie [45]; Panagiotopoulos and Reid [46];

Stryjek and Vera [21, 47]; Schwartzentruber et al. [48]; and Sandoval et al. [49]; have proposed modifications for the van der Waals mixing rules by introducing a composition–dependent term for a and leaving b parameter unchanged. Some examples are summarized in Table 4.5

Table 4.5: Composition–dependent mixing rules .

Author	a_{ij} in Eqn. 4.19
Adachi–Sugie [45]	$(a_{ii}a_{jj})^{1/2}(1 - l_{ij} + m_{ij}(x_i - x_j))$
Panagiotopoulos–Reid [46]	$(a_{ii}a_{jj})^{1/2}(1 - k_{ij} + (k_{ij} - k_{ji})x_i))$
Stryjek–Vera [47]	$(a_{ii}a_{jj})^{1/2}(1 - x_i k_{ij} - x_j k_{ji})$
Stryjek–Vera [21]	$(a_{ii}a_{jj})^{1/2}\left[1 - \dfrac{k_{ij}k_{ji}}{x_i k_{ij} + x_j k_{ji}}\right]$
Schwartzentruber [48]	$(a_{ii}a_{jj})^{1/2}\left[1 - k_{ij} - l_{ij}\dfrac{m_{ij}x_i - m_{ji}x_j}{m_{ij}x_i + m_{ji}x_j}(x_i + x_j)\right]$ $k_{ij} = k_{ji};\ l_{ij} = -l_{ji};\ m_{ji} = 1 - m_{ij}\ ;\ k_{11} = l_{11} = 0$
Sandoval [49]	$(a_{ii}a_{jj})^{1/2}(1 - (k_{ij}x_i + k_{ji}x_j)$ $-0.5(k_{ij} + k_{ji})(1 - x_i - x_j))$

A different approach was proposed by Deiters [56]. He introduced density dependence into the van der Waals mixing rules for simple fluids by applying a variable exponent δ for nonequiform particle distribution in mixtures

$$\epsilon\sigma^\delta = \sum\sum x_i x_k \epsilon_{ik}\sigma_{ik}^\delta \qquad (4.22)$$

$$\sigma^\delta = \sum \sum x_i x_k \sigma_{ik}^\delta \tag{4.23}$$

where

$$\delta = 3(1 - \xi^2) \tag{4.24}$$

The exponent can be obtained by integration of radial distribution function of rigid–sphere mixtures. This mixing rules improve calculations of phase equilibria in cryogenic mixtures, espetially near critical points. In 1987 Deiters [57] extended his mixing rules to nonspherical molecules.

Chapter 5

Development of new quantum corrections

5.1 Cubic cell model

In 1983, Deiters [53, 54] proposed a very useful and simple model to calculate the quantum effects in fluid phase of light molecules and atoms. The quantum correction can be applied in any classical equation of state which is separable into a repulsive and an attractive part. Therefore, all van der Waals type equations of state in Sec. 4.2 can be used to calculate the quantum effect.

This model presents a straightforward method for quantum corrections on translational partition function by using the "particle in a cubic box" energy spectrum. It was shown in Sec. 2.5 that translational motions of a particle in a cubic box are restricted, and the energy of this particle are discontinuous. Translational motions of molecules in a fluid under high pressure are also restricted. Each molecule is affected by the repulsive potentials of its neighbours which increase with increasing density, therefore, the translational energy is no longer continuous. At high densities the translational energy states are not closely spaced and the assumption used in Sec. 3.6 to calculate the translational partition function by integration (Eqn. 3.27) is no longer valid.

It was assumed that each molecule is restricted in a cubic cell by the repulsion of its neighbour molecules (Fig. 5.1). The eigenvalues of a particle in a cubic box of length R_0 were used

$$E = \frac{(n_x^2 + n_y^2 + n_z^2)h^2}{8mR_0^2} \tag{5.1}$$

It was assumed that the cell length R_0 is related to the free volume,

$$R_0 = 2\sqrt[3]{\frac{V_{\mathrm{f}}}{N}} \tag{5.2}$$

where V_{f} is the free volume, N stands for the number of molecules and the factor 2 accounts for cell overlapping.

The energy levels of Eqn. 5.1 and also Eqn. 3.20 were used to calculate the partition function of a molecule.

$$q_{\mathrm{trans}} = \Big[\sum_j \exp\big(-\frac{j^2 h^2}{8mkTR_0^2}\big)\Big]^3 = \Big[\sum_j \exp\big(-\frac{\pi}{4}j^2 y^2\big)\Big]^3 \tag{5.3}$$
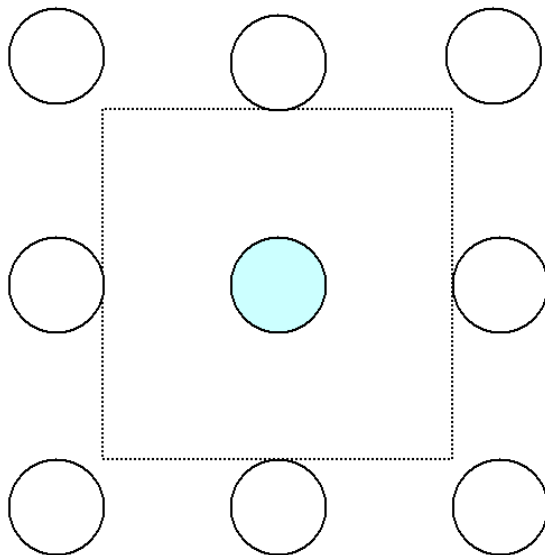
Figure 5.1: Cubic cell model.

In this equation y is reduced wavelength and is defined as

$$y = \frac{\Lambda}{R_0} \tag{5.4}$$

where Λ is thermal de Broglie wavelength,

$$\Lambda = \sqrt{\frac{h^2}{2\pi m k T}}. \tag{5.5}$$

The quantum mechanical partition function was obtained from the molecular partition function using Sec. 3.6 and Eqns. 3.23 and 3.32 and the assumption that there are $N/8$ distinct cells available for each molecule.

$$Q_{qu} = \frac{1}{N!}\left(\frac{N}{8}q_{trans}\right)^N Q_{int} = Q_{cl}\left[y \sum_j \exp\left(-\frac{\pi}{4}y^2 j^2\right)\right]^{3N}. \tag{5.6}$$

This correction function is expanded into a power series in y

$$\ln\left[y\ \sum_j\ \exp\left(-\frac{\pi}{4}y^2j^2\right)\right] = \sum_i\ r_iy^i \qquad (5.7)$$

for which the coefficients r_i are shown in Table 5.1

Table 5.1: Expansion coefficients of Deiters quantum correction function.

i	r_i	i	r_i
0	0	7	8.6632912449
1	-0.49995174927	8	-8.7278378272
2	-0.12867273248	9	5.7423465620
3	0.026360453309	10	-2.4445076274
4	-0.55253407160	11	0.64896811633
5	2.2409938208	12	-0.097758376489
6	-5.5702015921	13	0.006387718839

The cubic cell model is a good and straightforward method for prediction of thermodynamic properties of quantum fluids at high densities. However, the cell model is not suitable at low densities or high temperatures and overestimates the quantum effects. Furthermore, assuming a cubic form for the cell is unrealistic.

5.2 Spherical cell model

To remove the weaknesses of the cubic cell model we applied a more realistic model by assuming a spherical symmetric cell. We assumed that molecules of a high density fluid are confined in a approximately spherical cell formed by the repulsive potentials of its neighbouring molecules (cf. Fig. 5.2).

In (1997) Kohlbruch [64] used the same model for the calculation of quantum corrections on equations of state. However, some very coarse approximations and assumptions used in solving the equations, introduced some uncertainties and led on some instances even to unrealistic results.

Similar to the previous section, the one-particle partition function can be calculated by obtaining the energy eigenvalues of the present model. However, the spherical geometry of this model involves considerable mathematical complexity.
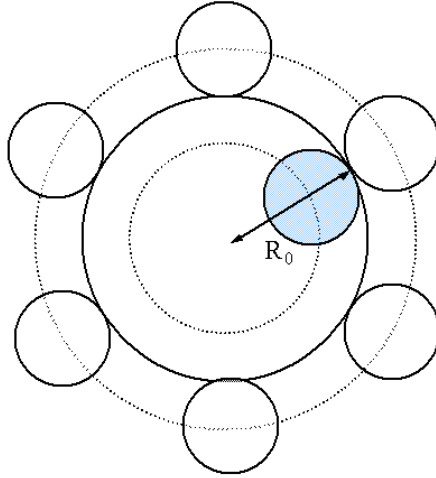

Figure 5.2: Spherical cell model.

The Schrödinger equation is solved in Sec. 2.6.1 for a particle in a spherical cell to obtain the energy spectrum. The potential energy function is assumed to be

$$V(r) = \begin{cases} 0 & \text{for } r < R_0 \\ \infty & \text{for } r \geq R_0 \end{cases}$$

where R_0 is the spherical cell radius which is related to the free volume V_f with the following relations

$$\frac{4}{3}\pi R_0^3 = g\frac{V_\text{f}}{N} \tag{5.8}$$

where the factor g accounts for cell overlapping.

According to calculations in Sec. 2.6.1 the energy eigenvalues are as follows

$$E_l = \frac{\hbar^2 (j_{l,n}^*)^2}{2mR_0^2} \qquad (5.9)$$

where $j_{l,n}^*$ denotes the nth roots of the j_l, and j_l is

$$j_l(x) = (-x)^l \left(\frac{1}{x} \frac{\mathrm{d}}{\mathrm{d}x} \right)^l \left(\frac{\sin(x)}{x} \right). \qquad (5.10)$$

We wish to compute the set of the first n zeros of the Bessel function for various integer orders l. A computer program in C was developed to calculate the $j_{l,n}^*$ set considering the following items

1. Eqn. 5.11, which gives the first zeros of j_ls with the different ls,

$$j_{l,1}^* \simeq (l + 1/2) + 1.85575(l + 1/2)^{1/3} + 1.03315(l + 1/2)^{-1/3}$$
$$-0.00397(l + 1/2)^{-1} - 0.0908(l + 1/2)^{-5/3} + \ldots \quad (5.11)$$

   where $v = (l + 1/2)$,

2. The nth zero for the spherical bessel function j_0.

$$j_0(x) = \frac{\sin(x)}{x} \qquad (5.12)$$

$$j_{0,n}^* = n\pi \qquad (5.13)$$

3. the recursion relation between successive spherical Bessel j functions,

$$j_{l+1}(x) = \frac{2l + 1}{x} j_l(x) - j_{l-1}(x) \qquad (5.14)$$

4. the fast 1-dimensional "regula falsi" iteration program which is used to solve a function in an interval containing only one zero. and finally,

5. a function which is used as an approximate increment. This function can be added to the previous zero to make an interval which the next zero is certainly situated inside the interval,

$$\text{incr}(n, l) = \frac{1}{n+1}\sqrt{l} + \left(\frac{0.1197}{(n+1)^3} - \frac{0.11576}{(n+1)^2} + \right.$$
$$\left. \frac{0.01559}{n+1} + .0007748 \right)l + 5.0 \qquad (5.15)$$

In other words, if we have computed a zero $j^*_{l,k-1}$, then the interval in which to search for the next zero, $j^*_{l,k}$ is from $(j^*_{l,k-1} + \delta)$ to $(j^*_{l,k} + \text{incr})$ where δ is a small number which is added to $j^*_{l,k-1}$ to make sure that the previous zero is not situated in the interval.

The zeros are calculated for $l \leq 300$ and $n \leq 300$, and are used to calculate the partition function.

5.3   Calculation of the partition function

Obtaining the molecular partition function (Sec. 3.6 and Eqns. 3.23 and 3.32), the quantum mechanical partition function can be calculated

$$q_{\text{trans}} = \sum_l \sum_n (2l+1) \, \exp\left(\frac{-\hbar^2 j^2_{l,n}}{2mkTR_0^2}\right) \qquad (5.16)$$

Introducing the thermal de Broglie wavelength Eqn. 5.5, and reduced wavelength y, Eqn. 5.4, to Eqn. 5.16 we obtain

$$q_{\text{trans}} = \sum_l \sum_n (2l+1) \, \exp\left(-\frac{1}{4\pi}y^2 j^2_{l,n}\right) \qquad (5.17)$$

where $(2l+1)$ term is the degeneracy, because for each l there exist $(2l+1)$ degenerate levels (with the same eigenvalue but different eigenfunctions) caused by solution of the spherical harmonics $Y_l^m(\theta, \phi)$ (Page 29 and App. C).

The partition function of a classical real gas is

$$Q_{\text{cl}} = \frac{1}{N!} \left(\frac{V_f}{\Lambda^3} \right)^N Q^{\text{int}} \tag{5.18}$$

where Q^{int} contains the contributions of the attractive potential and inner degrees of freedom. For the cell model we obtain

$$Q_{\text{qu}} = \frac{1}{N!} \left(\frac{N}{g} q \right)^N Q^{\text{int}} \tag{5.19}$$

substituting the Eqns. 5.8, 5.17 and 5.18 in the Eqn. 5.19, we obtain

$$
\begin{aligned}
Q_{\text{qu}} &= Q_{\text{cl}} \left[\frac{3}{4\pi} y^3 \sum_l \sum_n (2l+1) \exp\left(-\frac{1}{4\pi} y^2 (j_{l,n}^*)^2 \right) \right]^N \\
&= Q_{\text{cl}} \, q'^N \tag{5.20}
\end{aligned}
$$

using $j_{l,n}^*$ obtained from the C program in Sec. (5.2), the term in the square brackets, q',can be calculated numerically and its logarithm can be expanded into the power series in y. The results are shown in Table 5.2.

$$\ln q' = \ln \left[\frac{3}{4\pi} y^3 \sum_l \sum_n (2l+1) \exp\left(-\frac{1}{4\pi} y^2 j_{l,n}^2 \right) \right] = \sum_{i=1}^{i=13} r_i y^i \tag{5.21}$$

The r_i coefficients are shown in Table 5.3

The expression $\sum_{i=1}^{13} r_i y^i$ of this work are compared with the same expression from the cubic cell model (Table 5.1) and the results of Kohlbruch [64] in Fig. 5.3.

The expression $\sum_{i=1}^{13} r_i y^i$ must vanish at $y = 0$ which is the classical limit.

5.4   Thermodynamic properties

From the quantum corrected canonical partition function, The Helmholtz free energy of the system can be calculated. The quantum corrected

Table 5.2: The quantum correction to the partition function, ln q' (see Eqn. 5.20) as a function of the reduced wavelength y.

y	ln q'	y	ln q'
0.100000	-0.076248	0.540000	-0.445342
0.120000	-0.091805	0.560000	-0.463604
0.140000	-0.107468	0.580000	-0.482010
0.160000	-0.123237	0.600000	-0.500564
0.180000	-0.139116	0.620000	-0.519268
0.200000	-0.155104	0.640000	-0.538123
0.220000	-0.171204	0.660000	-0.557132
0.240000	-0.187417	0.680000	-0.576299
0.260000	-0.203745	0.700000	-0.595624
0.280000	-0.220189	0.720000	-0.615112
0.300000	-0.236751	0.740000	-0.634764
0.320000	-0.253433	0.760000	-0.654583
0.340000	-0.270236	0.780000	-0.674573
0.360000	-0.287162	0.800000	-0.694735
0.380000	-0.304213	0.820000	-0.715073
0.400000	-0.321390	0.840000	-0.735591
0.420000	-0.338697	0.860000	-0.756289
0.440000	-0.356133	0.880000	-0.777173
0.460000	-0.373702	0.900000	-0.798245
0.480000	-0.391406	0.920000	-0.819509
0.500000	-0.409245	0.940000	-0.840967
0.520000	-0.427224	0.960000	-0.862624
0.540000	-0.445342	0.980000	-0.884482

Table 5.3: Expansion coefficients of quantum correction function based on the spherical cell model

i	r_i	i	r_i
0	0	7	3.115526848
1	-0.7563398333	8	-0.8260182969
2	-0.0167642267	9	1.092423845
3	-0.6393742663	10	-0.5892323173
4	1.475145308	11	-5.552969409
5	-0.8803506078	12	7.524010628
6	-2.117627725	13	-2.735233166
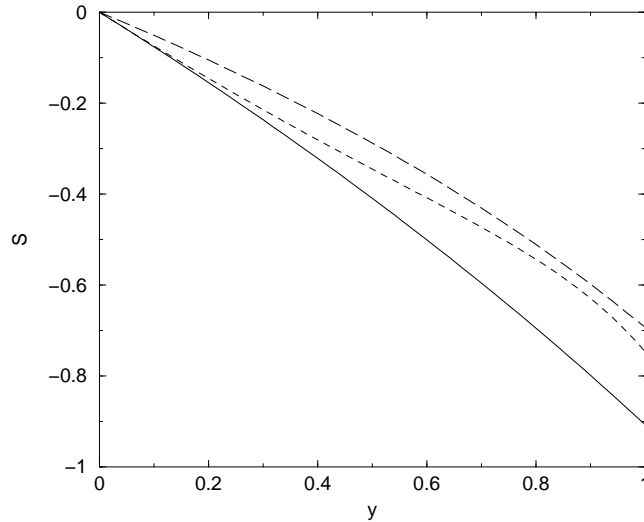
Figure 5.3: Series expansion $\sum_{i=1}^{13} r_i y^i$ based on the spherical cell model (solid line), cubic cell model (long–dashed line), and $\sum_{i=1}^{10} r_i y^i$ in Kohlbruch's result (dashed line.)

Helmholtz free energy, and a van der Waals type equation of state which can be separated into repulsive and attractive parts

$$p = p_{\text{rep}} + p_{\text{att}} \tag{5.22}$$

can be readily used to calculate the quantum effects in the equation of state.

Using Eqn. 3.12 and canonical partition function Eqn. 5.20 obtained in Sec. 5.3, the Helmholtz free energy can be obtained as

$$A_{\text{qu}} = -kT \ln Q_{\text{qu}} = A_{\text{cl}} - RT \sum_{i=1}^{i=13} r_i y^i \qquad (5.23)$$

and

$$p_{\text{qu}} = -\left(\frac{\partial A_{\text{qu}}}{\partial V_{\text{m}}}\right)_T = p_{\text{cl}} - p_{\text{rep}} \sum_{i=1}^{13} i r_i y^i. \qquad (5.24)$$

5.5 Low density and high temperature corrections

At low densities or high temperatures the cell model is not suitable for description of fluids, because the molecules are not totally restricted to their hypothetical cells.

The cell walls act as a barrier for the particle contained in the cell. In Sec. 2.6.1, the potential energy was assumed to be infinite for $r \geq R_0$; however, there exist no infinite potentials in nature. We therefore propose to use cell walls of finite height, which allow a particle to escape from its cell. If a particle has less energy than the energy barrier, the cell walls can be considered as an infinite potential barrier for the particle, under such conditions the particle has not enough energy to run out of the cell, neglecting the tunnel effect. They can be considered as quantum particles. At higher temperature, some molecules have more energy than the potential energy barrier and are no longer quantum particles, they can freely move and leave the cell. Decreasing the density produces the same effect. At lower densities, the repulsion potential energy, which is the cell energy barrier, decreases. The number of classical particles increases with increasing temperature and decreasing density.

The Boltzmann distribution can be used to calculate the number of free particles which have more energy than the barrier energy of the cell. The

Boltzmann distribution is a classical distribution function for distribution of an amount of energy between identical particles. The probability that an entity has an energy between E and $E+\mathrm{d}E$ is given by the Boltzmann probability distribution function

$$P(E) = C\mathrm{e}^{(-E/k_\mathrm{B}T)} \tag{5.25}$$

where C is normalization constant, assuming that an entity can have an energy between zero and infinity, $C = 1/kT$. Then, the number of classical particles (n) which have more energy than a given energy E_0 (energy barrier), is obtained as

$$n = \frac{N}{k_\mathrm{B}T}\exp\left(-\frac{E}{k_\mathrm{B}T}\right) \tag{5.26}$$

In order to correct the translational partition function at high temperature and low density limit, it is separated into two parts, a classical, and a quantum part

$$Q_\mathrm{total} = Q_{\mathrm{cl},n}\ Q_{\mathrm{qu},(N-n)}\ Q_\mathrm{int} \tag{5.27}$$

where $Q_{\mathrm{cl},n}$ is partition function for n classical particles, and $Q_{\mathrm{qu},(N-n)}$ is partition function for $(N-n)$ quantum particles. Using Stirling's approximation, (for N large)

$$\ln N! = N\ln N - N \tag{5.28}$$

and substituting Eqns. 5.8 and 5.5, Eqn. 5.18 can be written as

$$\begin{aligned}
Q_{\mathrm{cl},n} &= \frac{1}{n!}\left(\frac{V_\mathrm{f}}{\Lambda^3}\right)^n Q_{\mathrm{int},n} \\
&= \mathrm{e}^n\left(\frac{V_\mathrm{f}}{n\Lambda^3}\right)^n Q_{\mathrm{int},n} = \mathrm{e}^n\left(\frac{4\pi}{3g}\frac{1}{y^3}\right)^n Q_{\mathrm{int},n}
\end{aligned} \tag{5.29}$$

and Q_qu for $(N-n)$ quantum particle can be obtained as

$$\begin{aligned}
Q_{\mathrm{qu},(N-n)} &= \frac{1}{(N-n)!}\left(\frac{(N-n)}{g}q_\mathrm{trans}\right)^{(N-n)} Q_{\mathrm{int},(N-n)} \\
&= \mathrm{e}^{(N-n)}\left(\frac{q_\mathrm{trans}}{g}\right)^{(N-n)} Q_{\mathrm{int},(N-n)}
\end{aligned} \tag{5.30}$$

Substituting Eqns. 5.29 and 5.30 into Eqn. 5.27, the total translational partition function is calculated

$$Q_{\text{total}} = \left(\frac{4\pi}{3g}\frac{\text{e}}{y^3}\right)^n \left(\frac{\text{e}\, q_{\text{trans}}}{g}\right)^{(N-n)} \left(\frac{3g}{4\pi}\frac{y^3}{\text{e}}\right)^N Q_{\text{cl}} \qquad (5.31)$$

finally

$$Q_{\text{total}} = \left(\frac{3}{4\pi}y^3 q_{\text{trans}}\right)^{(N-n)} Q_{\text{cl}} \qquad (5.32)$$

where

$$y = \frac{k_1 \Lambda}{(V_{\text{f}}/N)^{1/3}}. \qquad (5.33)$$

and $k_1 = (4\pi/3g)^{1/3}$. The free volume is obtained by an equation of state (Eqn. 4.12) proposed by Deiters [50, 51]

$$V_{\text{f}} = V \exp\left(cc_0 \frac{3\xi^2 - 4\xi}{(1-\xi)^2}\right) \qquad (5.34)$$

Applying Eqns. 5.5 and 5.34 into Eqn. 5.33,

$$y^2(T, \rho, \sigma) = \frac{h^2 k_1^{2/3}}{2\pi m kT} \rho^{2/3} \left[\exp\left(-cc_0 \frac{3\xi^2 - 4\xi}{(1-\xi)^2}\right)\right]^{2/3} \qquad (5.35)$$

for $y = y_0$

$$k_{\text{B}} T_{\text{ref}}^* = \frac{h^2 k_1^{2/3}}{2\pi m y_0^2} \rho^{2/3} \exp\left(-\frac{2}{3} cc_0 \frac{3\xi^2 - 4\xi}{(1-\xi)^2}\right) = E_{\text{ref}} \qquad (5.36)$$

We choose the energy E_{ref} as the barrier energy of the cell.

$$\frac{E_{\text{ref}}}{k_{\text{B}} T} = \frac{y^2(\rho, T, \sigma)}{y_0^2} \qquad (5.37)$$

The number of classical particles can be obtained by integrating Eqn. 5.26

$$n = \frac{N}{k_{\text{B}} T} \int_{E_{\text{ref}}}^{\infty} \exp\left(-\frac{E}{k_{\text{B}} T}\right) dE \qquad (5.38)$$

71

and

$$n = \frac{N}{k_{\mathrm{B}}T}\Big(- kT\exp\Big(- \frac{E}{k_{\mathrm{B}}T}\Big)\Big)\Big|_{E_0}^{\infty} \tag{5.39}$$

$$n = N\exp\Big(- \frac{E_{\mathrm{ref}}}{k_{\mathrm{B}}T}\Big) \tag{5.40}$$

or equivalently

$$n = N\exp\Big(- \frac{y^2(\rho, T, \sigma)}{y_0^2}\Big) \tag{5.41}$$

Substituting Eqn. 5.41 into the logarithm of Eqn. 5.31 yields

$$\ln Q_{\mathrm{total}} = (N - n)\ln\Big(\frac{3}{4\pi}y^3 q_{\mathrm{trans}}\Big) + \ln Q_{\mathrm{cl}} \tag{5.42}$$

$$\ln Q_{\mathrm{total}} = N\Big(1 - \exp\Big(- \frac{y^2(\rho, T, \sigma)}{y_0^2}\Big)\Big)\ln\big(\frac{3}{4\pi}y^3 q_{\mathrm{trans}}\big) + \ln Q_{\mathrm{cl}} \tag{5.43}$$

and

$$\ln Q_{\mathrm{total}} = N\Big(1 - \exp\Big(- \frac{y^2(\rho, T, \sigma)}{y_0^2}\Big)\Big)\sum_{i=1}^{i=13} r_i y^i + \ln Q_{\mathrm{cl}} \tag{5.44}$$

finally, defining $\alpha = 1/y_0^2$ and $X_i(y) = \sum_{i=1}^{i=13} r_i y^i$

$$\ln Q_{\mathrm{total}} = N(1 - \mathrm{e}^{-\alpha y^2})X_i(y) + \ln Q_{\mathrm{cl}}. \tag{5.45}$$

Chapter 6

Results and discussion

Using the ThermoC package [55], calculations of fluid phase coexistence curves, pressure isotherms, and critical parameters have been done. ThermoC is a modular program package for the calculation of arbitrary thermodynamic properties of pure fluid and binary fluid mixtures with any equation of state or mixing rule. Calculation of all kinds of fluid phase equilibria and solid–fluid phase equilibria are possible by ThermoC package. (App. D)

The ThermoC program package has been extended to calculate the fluid phase equilibria of quantum fluids using the new spherical cell model and high temperature and low density limit corrections.

The Deiters equation of state [50, 51], which is introduced in Sec. 4.3, has been applied to demonstrate the new quantum corrections. This equation of state gives a very good results for classical gases.

6.1   Expansion coefficients r_i

The expansion coefficients of quantum correction function for the spherical cell model (r_i) which are calculated in Sec. 5.3, are tabulated in Table 5.3. Addition of the high temperature and low density limit correction function to the ($\sum_{i=1}^{13} r_i y^i$) expression leads to a curve which shows less quantum effect at high temperature or low density limit ($y \rightarrow 0$) than the expression without the corrections. Increasing α (which is defined as $1/y_0^2$ and is a measure of the potential energy barrier of the cell), the quantum effects for the smaller values of y are decreased. In Fig. 6.1, the ($\sum_{i=1}^{13} r_i y^i$) expression is compared with (($1 - e^{-\alpha y^2}$) $\sum_{i=1}^{i=13} r_i y^i$) for the different values of α.

The same correction function can be applied for the expansion coefficients (r_i) for the cubic cell model (Table 5.1) and shows same effects (Fig. 6.2).

Comparison between X_is for the cubic and the spherical cell model shows that in the spherical model, calculated quantum effects are larger than in the cubic model (Fig. 6.3 .)
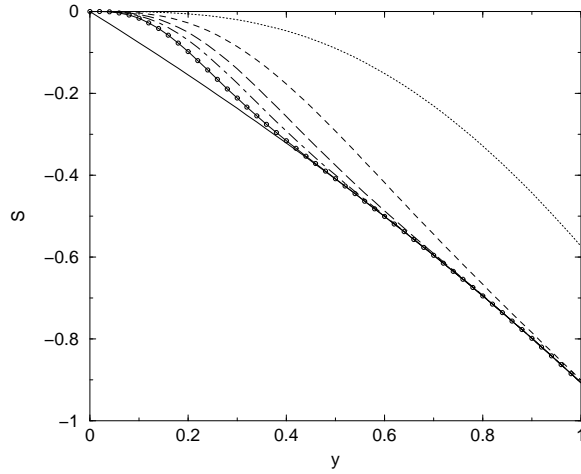
Figure 6.1: Comparison of $X_i(y)$ from spherical cell model (solid line), with $(1 - e^{-\alpha y^2})X_i(y)$ expressions for the different αs, $\alpha = 1$ (dotted line), $\alpha = 5$ (dashed line), $\alpha = 10$ (long dashed), $\alpha = 15$ (dot-dashed), and $\alpha = 25$ (circle-line).
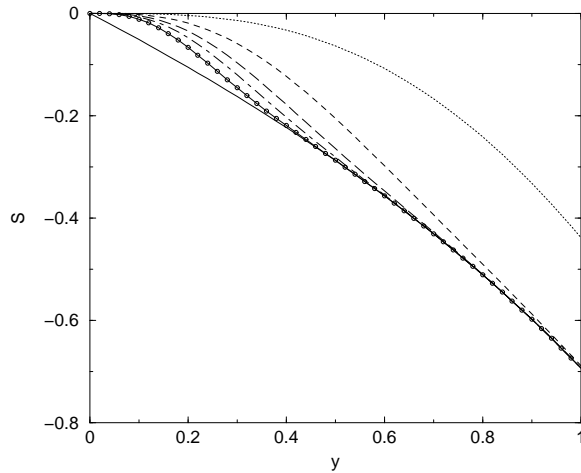

Figure 6.2: Comparison of $X_i(y)$ from cubic cell model (solid line), with $(1 - e^{-\alpha y^2})X_i(y)$ expressions for the different αs, $\alpha = 1$ (dotted line), $\alpha = 5$ (dashed line), $\alpha = 10$ (long dashed), $\alpha = 15$ (dot-dashed), and $\alpha = 25$ (circle-line).
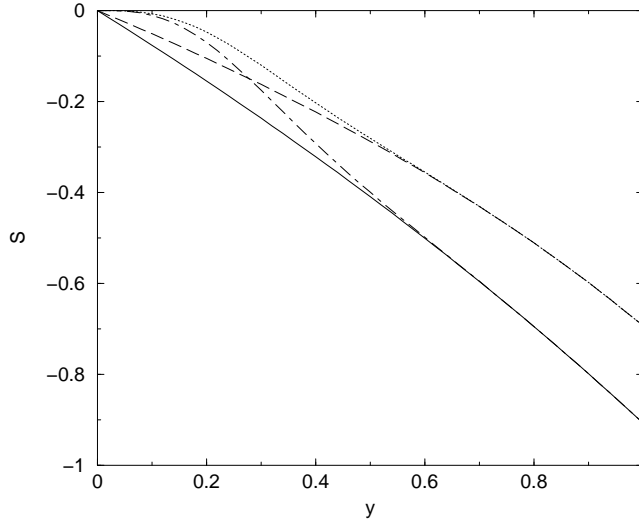
Figure 6.3: $X_i(y)$ (solid line) and $(1 - e^{-\alpha y^2})X_i(y)$ with $\alpha = 15$ (dot-dashed) for spherical cell model are compared with $X_i(y)$ (long dashed) and $(1 - e^{-\alpha y^2})X_i(y$ for the same value of α (dotted line) in the cubic cell model.

6.2   Pure fluids

6.2.1   Neon

Quantum corrected equation of state

The coexistence curve has been calculated for neon using the Deiters equation of state with the new quantum correction functions. Fig. 6.4 shows the results of the Deiters equation of state without quantum corrections, and with cubic cell model correction functions, and compares with experimental data.

The results of new model are in an excellent agreement with experiment, and an improvement in comparison with cubic cell model is observed.

On the other hand, the vapor–liquid coexistence curve of the new model is compared with the simulation results.
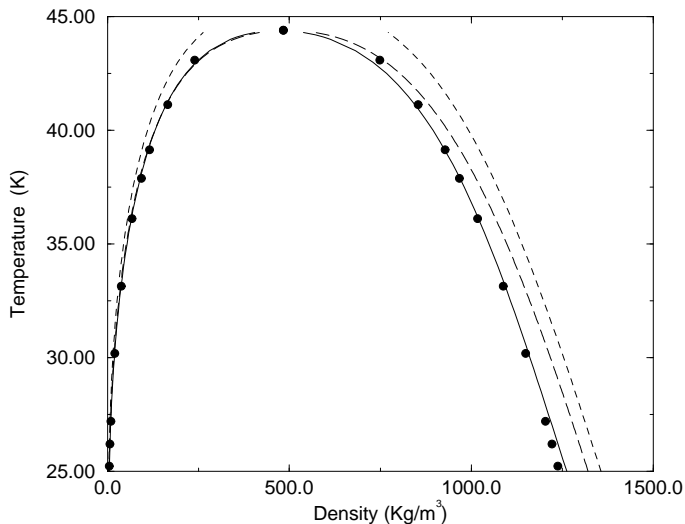
Figure 6.4: Densities of coexisting phases of neon. Comparison of Deiters equation of state with the cubic cell model results (long-dashed line), without quantum corrections (dashed line), with spherical cell model for $\alpha = 9$ (solid line), and experiment (•))

Global simulations

Global simulation [68] uses the *ab initio* potential interactions in computer simulations to obtain fluid phase properties without using any empirical parameters.

Cybulski and Toczylowski [70] reported an *ab initio* potential for neon using the CCSD(T) level of theory and several correlation consistent basis sets. Results of the aug-cc-pVQZ (avqz) and the aug-cc-pV5Z (av5z) basis sets were extrapolated by $(1/X^3)$ method to obtain the basis set limit (av45z) of the interaction energies [65][App. E].

The potential data have been fitted using the analytical representation of Korona et. al. [69]

$$\phi(R) = Ae^{-\alpha R + \beta R^2} + \sum_{n=3}^{8} f_{2n}(R, b) \frac{C_{2n}}{R^{2n}} \qquad (6.1)$$

where A, α, β and b denote adjustable parameters, C_{2n} denotes a dispersion

coefficient, and f_{2n} is the damping function of Tang and Toennies [71]

$$f_{2n}(R, b) = 1 - e^{-bR} \sum_{k=0}^{2n} \frac{(bR)^k}{k!} \qquad (6.2)$$

Gibbs ensemble Monte Carlo simulations [66] were performed to calculate the vapor–liquid phase equilibria of neon [65]. Effects of three-body interactions were taken into account using Axilrod–Teller [67] (AT) triple-dipole potential. Results of the simulation show that addition of the AT potential to the total energy leads to a better agreement with experimental data; however, there are still large descrepancies especially in the liquid branch which are mainly due to the quantum effects.

Results of the simulations, Deiters equation of state with and without quantum corrections, and experimental data are shown in Figs. 6.5 and 6.6.
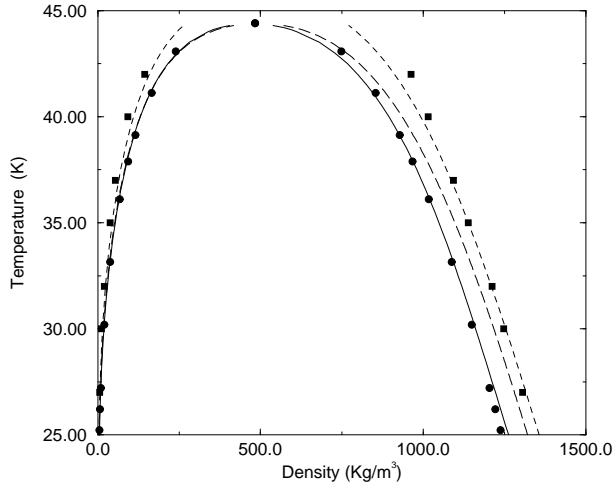

Figure 6.5: Densities of coexisting phases of neon. Comparison of Deiters equation of state with the cubic cell model results (long-dashed line), without quantum corrections (dashed line), with spherical cell model for $\alpha = 9$ (solid line), experiment (•) and GEMC simulation results with the av45z plus AT potentials (■)

Addition of AT potential to the total energy makes a better agreement with experiment and the results are very close to the Deiters equation
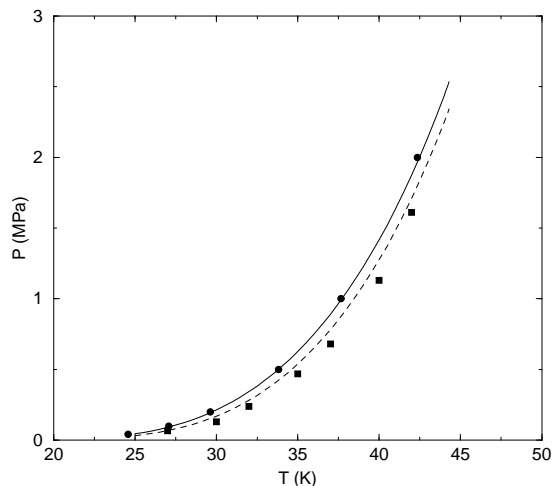
Figure 6.6: Comparison of vapor pressures for neon: Deiters equation of state without quantum corrections (dashed line), with spherical cell model for $\alpha = 9$ (solid line), experiment (•) and GEMC simulation results with the av45z plus AT potentials (■)

of state without quantum corrections. It shows that deviations from the experimental data are caused by quantum effects and can be corrected by inclusion of the new quantum corrections.

6.2.2 Hydrogen

Hydrogen shows more pronounced quantum effects than neon (Tabel 1.1). The coexistence curve of hydrogen has been calcuated using Deiters equation of state with the new quantum corrections, and the results have been compared with the experiment, and the Deiters equation of state with cubic cell model quantum corrections. As seen in Figs. 6.7 and 6.8 the results of cubic cell model improves the result but there are still large discrepancies in the liquid branch, the new model improves the results and leads to a good agreement with experiment.

The vapor pressure curve of hydrogen is shown in Fig. 6.9. Comparison between the new and the old model shows that the new model improves the results especially at lower temperatures.
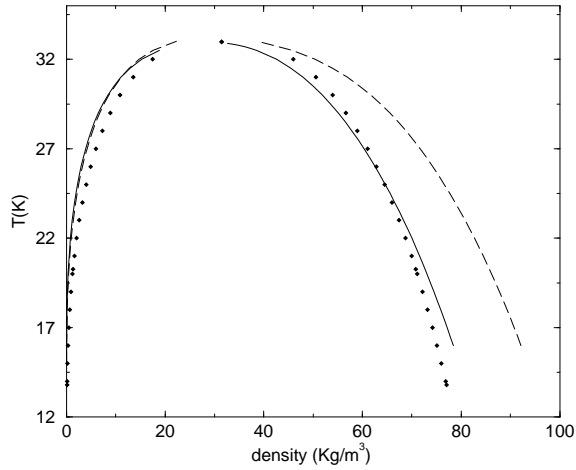
Figure 6.7: Densities of coexisting phases of hydrogen. Comparison of Deiters equation of state with the cubic cell model results (long-dashed line), with spherical cell model for $\alpha = 50$ (solid line), and experiment ($\bullet$))
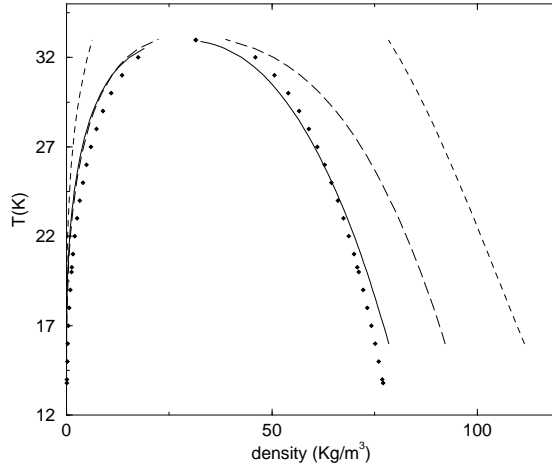

Figure 6.8: Densities of coexisting phases of hydrogen. Comparison of Deiters equation of state with the cubic cell model results (long-dashed line), without quantum corrections (dashed line), with spherical cell model for $\alpha = 50$ (solid line), and experiment ($\bullet$))
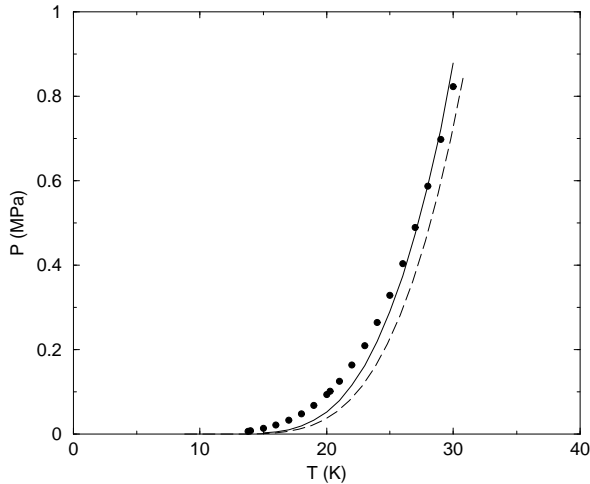
80

Figure 6.9: Comparison of vapor pressures for hydrogen , for Deiters equation of state with the cubic cell model results (long-dashed line), with spherical cell model for $\alpha = 50$ (solid line), and experiment ($\bullet$)

6.2.3 Methane

The vapor–liquid coexistence curve for methane shows rather small quantum effects (Table 1.1). The cubic cell corrections produce a good agreement with experimental data; however, in the liquid branch there exist some deviations. It is shown in Fig. 6.10 that results of the new model have an excellent agreement with the experimental data. The results of the spherical cell model with high temperature and low density corrections are not distinguishable from the experimental results. The vapor pressure results of both models, (as shown in Fig. 6.11) are in a very good agreement with the experimental vapor pressures.
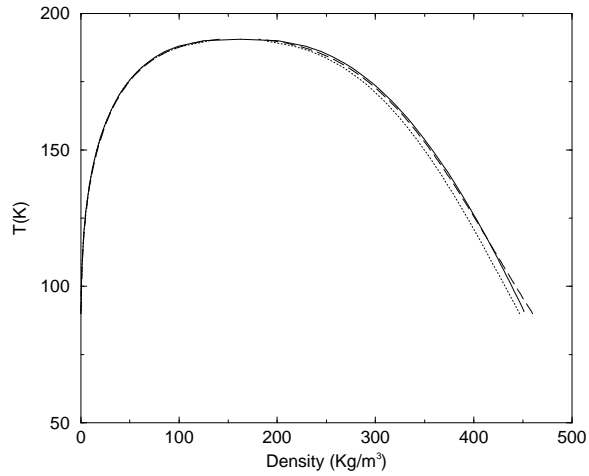
Figure 6.10: Densities of coexisting phases of methane. Comparison of Deiters equation of state with the cubic cell model results (dotted line), with spherical cell model for $\alpha = 100$ (long-dashed line), and experiment (solid line))

Figure 6.11: Comparison of vapor pressures of methane, Deiters equation of state with the cubic cell model results (dotted line), with spherical cell model for $\alpha = 100$ (long-dashed line), and experiment (solid line))
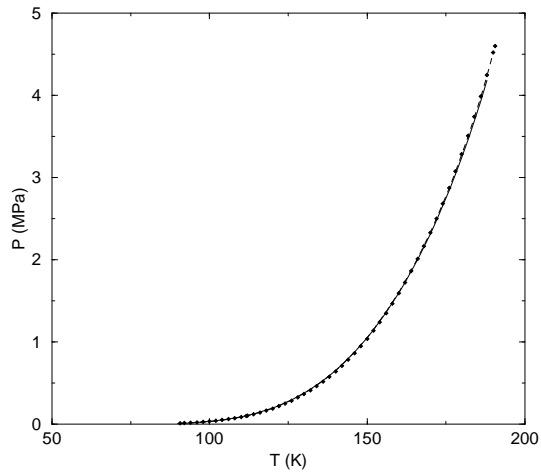
6.2.4 Nitrogen

In the case of nitrogen (such as methane), results of the cubic cell model are in a good agreement with the experiment. However, the results of the new model are in excellent agreement with the experimental data. The vapor–liquid coexistence curve and the vapor pressure data are shown in Figs. 6.12 and 6.13. The α parameter in this case is in the range of 300 ± 20, which is three times the α in the case of methane. It is probably due to the higher repulsive potentials between nitrogen molecules than the methane molecules.
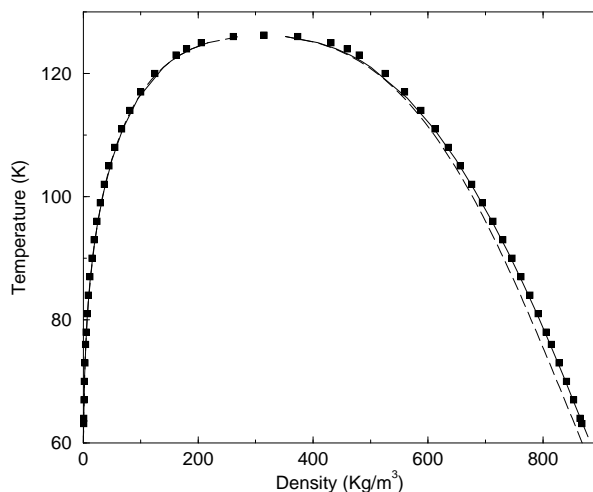

Figure 6.12: Densities of coexisting phases of nitrogen. Comparison of Deiters equation of state with the cubic cell model results (dashed line), with spherical cell model for $\alpha = 300$ (■), and experiment (solid line).
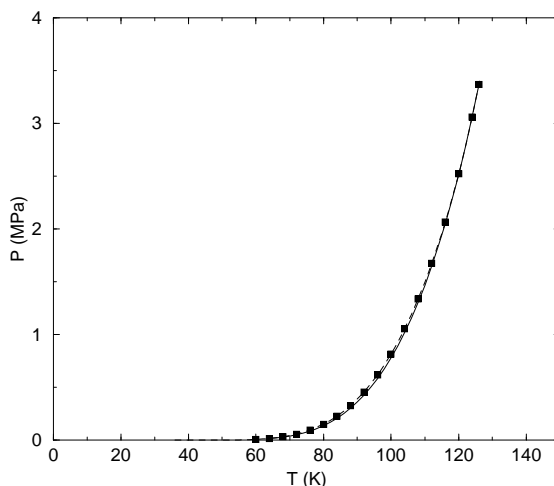
Figure 6.13: Comparison of vapor pressures of nitrogen, Deiters equation of state with the cubic cell model results (dashed line), with spherical cell model for $\alpha = 300$ (■), and experiment (solid line)).

6.3 Binary mixtures

A density-dependent mixing rule proposed by Deiters [56] was used for the calculation of fluid phase equilibria of binary mixtures of quantum fluids. The mixing rules are obtained by introducing a variable exponent into the van der Waals mixing rules to account for the non-equiform particle distribution in mixtures of unlike molecules (Sec. 4.4.1). The vapor–liquid co-existence curves for the binary mixtures of neon–argon, and neon–krypton for several different isotherms have been calculated.

6.3.1 Neon–Argon

The p–x–y phase equilibria of the neon–argon system have been calculated for 95.82 K, 101.94 K, 110.78 K, 121.36 K, and 129.93 K isotherms.

As seen in Fig. 6.14, at 95.82 K isotherm, the results of the new model are in better agreement with experimental data than the old model. The best results were obtained with $\alpha = 120$.

For the isotherm at 101.94 K, which is shown in Fig. 6.15 the results of the new model are in excellent agreement with experiment, and show significant improvements in comparison with the cubic cell model.It was found that $\alpha = 95$ gives the best results at this isotherm.

At 110.78 K isotherm, the old model has good results, however the new model improves the results in the right branch of the isotherm which are shown in Fig. 6.16. $\alpha = 45$ gives the best results.

The next two isotherms for the neon–argon mixtures are at 121.36 K, and 129.93 K, which are shown in Figs. 6.17 and 6.18 respectively. The new model shows improvements in both isotherms in the right (liquid) branch in comparison with the old model. The calculated pressures near the critical region are in better agreement with experimental data than with the old model. The α parameter at 121.36 K isotherm is 10, but in the case of 129.93 K isotherm, the α parameter is nearly zero which means that quantum effects calculated by the spherical cell model is nearly zero. It can be seen in Fig. 6.18 that old model overestimates the quantum effects at this isotherm, but the new model overcomes this deficiency.

Figure 6.14: The Ne-Ar system at 95.82 K. Comparison of the new model with $\alpha = 120$ (solid line), the old model (long-dashed) , and experiment ($\bullet$)
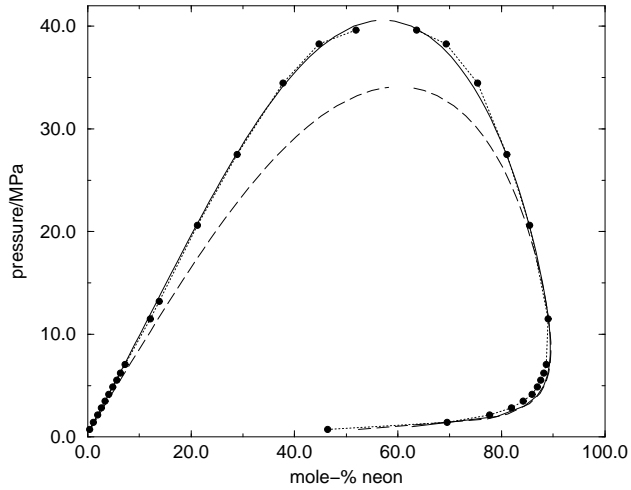
Figure 6.15: The Ne-Ar system at 101.94 K Comparison of the new model with $\alpha = 95$ (solid line), the old model (long-dashed), and experiment (•)
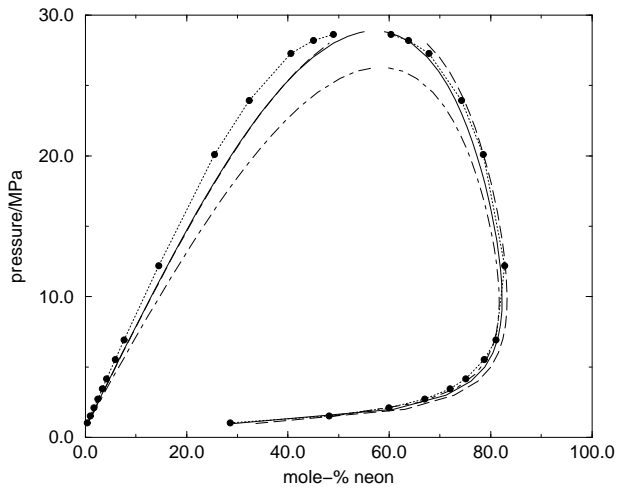
Figure 6.16: The Ne-Ar system at 110.78 K Comparison of the equation of state without quantum corrections (dot-dashed), new model with $\alpha = 45$ (solid line), the old model (long-dashed), and experiment (•)
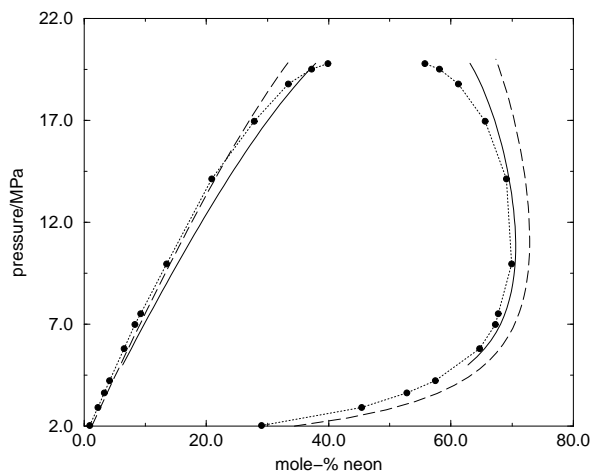
Figure 6.17: The Ne-Ar system at 121.36 K Comparison of the new model with $\alpha = 10$ (solid line), the old model (long-dashed), and experiment ($\bullet$)
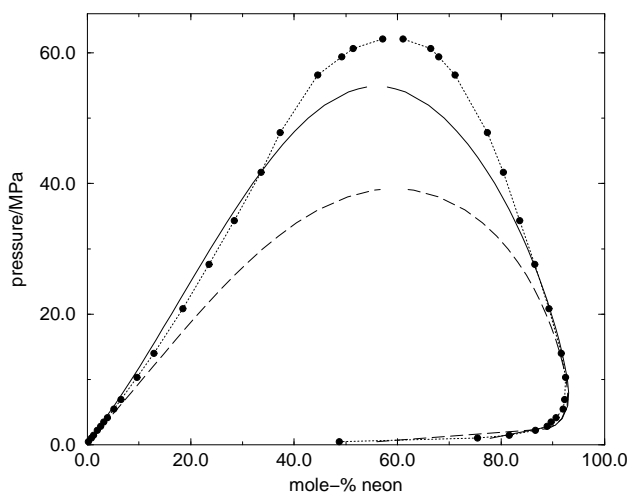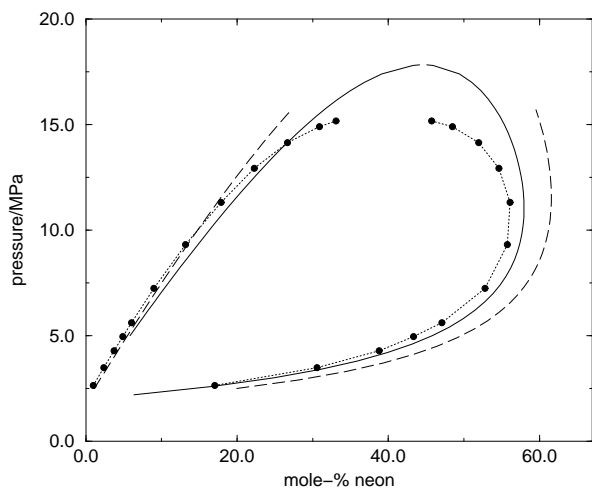

Figure 6.18: The Ne-Ar system at 129.93 K Comparison of the new model with $\alpha = 0$ (solid line), the old model (long-dashed), and experiment ($\bullet$)

87

6.3.2 Neon–Krypton

The p–x–y phase equilibria of the neon–krypton system have been calculated at three isotherms 133.15 K, 166.15 K, and 178.15 K.

The results are shown in Figs. 6.19, 6.20, and 6.21. An improvement is seen in the liquid branch of the first isotherm, 133.15 K by the new model, in comparison with the old model.

In the other two isotherms, the results of the new model show a better agreement with experiment. The α parameter is zero for these two isotherms. As the neon–argon case, the new model corrects the overestimation of the old model at higher temperatures.

Figure 6.19: The Ne-Kr system at 133.15 K. Comparison of the new model with $\alpha = 10$ (solid line), the old model (long-dashed), and experiment ($\bullet$-line)

The results show that the new model leads to a better agreement with the experiment than the cubic cell model.

Figure 6.20: The Ne-Kr system at 166.15 K. Comparison of the new model with $\alpha = 0$ (solid line), the old model (long-dashed), and experiment (•-line)

Figure 6.21: The Ne-Kr system at 178.15 K. Comparison of the new model with $\alpha = 0$ (solid line), the old model (long-dashed), and experiment (•-line)
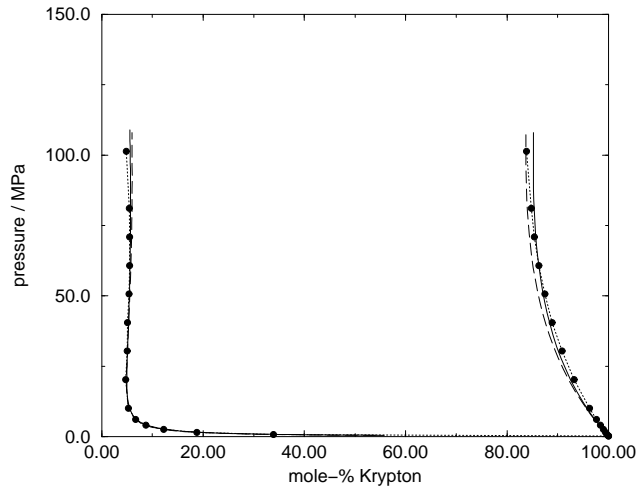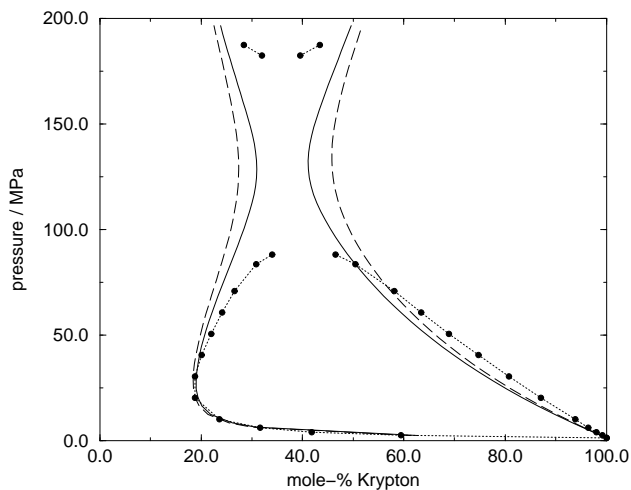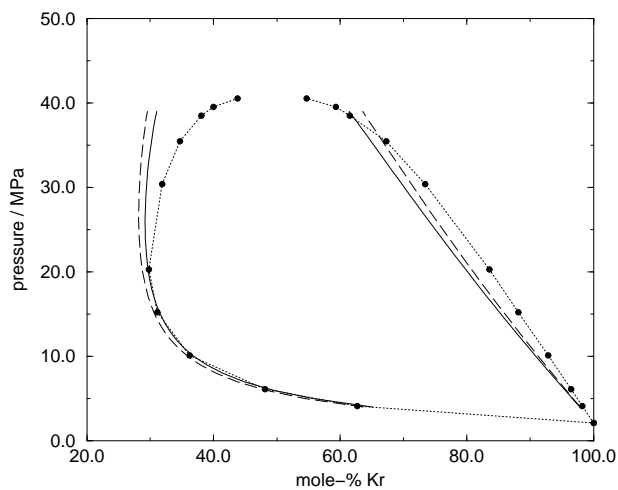
Chapter 7

Conclusion

The spherical cell model was used to calculate the translational energy eigenvalues of the system. The discontinuous energy spectrum was used to calculate the translational partition function for a molecule. Using statistical mechanical relations, the quantum corrected canonical partition function was calculated. A quantum correction function was obtained with a simple analytical form, which is applicable to any van der Waals type equation of state.

The new correction function was obtained to remove the weaknesses of the older cell model in the high temperature and low density limit. It is a function of temperature, molar mass, and the distance characteristic parameter (σ). It contains a physically meaningful adjustable parameter, (y_0), which can be considered as "reference reduced wavelength".

The correction functions were applied to the Deiters equation of state which has resonably good results in the classical limit.

The quantum effects in fluid phase equilibria of several pure systems namely, neon, hydrogen, nitrogen, and methane and two binary mixtures, neon–argon, and neon krypton were studied. The results are in a very good agreement with experiment.

A comprehensive investigation on predictions of phase equilibria for pure neon including simulations was reported. Inclusion of correction functions to the equation of state leads to an excellent agreement with experiment. On the other hand, the results of the simulations with accurate potentials show deviations from experiment. The results of the equation of state with and without quantum corrections suggest that the discrepancies in simulation results are due to quantum effects.

Fluid phase equilibria of the binary mixtures of neon–argon, and neon krypton were obtained for several isotherms using Deiters equation of state and a density dependent mixing theory. The results of the new model show good agreement with experiment. The addition of the high-temperature limit correction function to the cell model results removes the deficiencies of the cell model.

Appendix A

Series solution of the Bessel equation

The Bessel equation has the form ([3])

$$\frac{\mathrm{d}^2 u}{\mathrm{d}x^2} + \frac{1}{x}\frac{\mathrm{d}u}{\mathrm{d}x} + \left(1 - \frac{m^2}{x^2}\right)u = 0. \tag{A.1}$$

Expanding around the regular singular point $x = 0$ we obtain [3]

$$u(x) = x^\alpha [1 + \sum_1^\infty u_j x^j]. \tag{A.2}$$

Substitution of A.2 in the A.1, and multyplying by x^2, we obtain

$$x^\alpha [\alpha(\alpha - 1) + \sum_1^\infty (\alpha + j)(\alpha + j - 1)u_j x^j]$$

$$+ x^\alpha [\alpha + \sum_1^\infty (\alpha + j)u_j x^j]$$

$$+ x^\alpha [x^2 + \sum_1^\infty u_j x^{j+2} - m^2 - m^2 u_j x^j] = 0 \tag{A.3}$$

After equating coefficients of successive powers of x we obtain

$$\alpha(\alpha - 1) + \alpha - m^2 = 0, \quad \alpha = \pm m, \tag{A.4}$$

$$[\alpha(\alpha + 1) + \alpha + 1 - m^2]u_1 = 0, \tag{A.5}$$

$$[(\alpha + 2)(\alpha + 1) + \alpha + 2 - m^2]u_2 + 1 = 0, \tag{A.6}$$

$$\vdots$$

$$[(\alpha + j)(\alpha + j - 1) + \alpha + j - m^2]u_j + u_{j-2} = 0. \tag{A.7}$$

Using Eqns. A.4, Eqn. A.5 can be written as

$$(2\alpha + 1) = 0 \tag{A.8}$$

94

therefore $u_1 = 0$ for all values of α except for $\alpha = 1/2$, but we can take $u_1 = 0$ even for $\alpha = 1/2$. Therefore, the recursion relation A.7 becomes

$$u_1 = u_3 = u_5 = \ldots = u_{2n+1} = \ldots = 0. \tag{A.9}$$

Using $\alpha^2 = m^2$, Eqn. A.7 can be rewritten in the form

$$u_{2j} = -\frac{u_{2(j-1)}}{(2j+\alpha)^2 - m^2} = -\frac{u_{2(j-1)}}{4j(j+\alpha)}. \tag{A.10}$$

After applying Eqn. A.10 repeatedly and decreasing $u_{2(j-1)}$ to u_0, we obtain

$$u_{2j} = (-1)^2 \frac{u_{2(j-2)}}{4j(j-1)(j+\alpha)(j+\alpha-1)}$$
$$= \frac{(-1)^j \Gamma(1+\alpha)}{2^{2j} j! \Gamma(j+\alpha+1)} u_0, \tag{A.11}$$

where Γ is the gamma function and $u_0 = 1$. Substituting Eqns. A.9 and A.11 into A.2 we find two solutions.

$$u_x = \begin{cases} x^m \sum_0^\infty \frac{\Gamma(m+1)(-1)^r}{2^{2r} r! \Gamma(r+m+1)} x^{2r} \\ \\ x^{-m} \sum_0^\infty \frac{\Gamma(-m+1)(-1)^r}{2^{2r} r! \Gamma(r-m+1)} x^{2r} \end{cases}$$

Multiplying by $2^{\mp m}/\Gamma(\mp m+1)$ we obtain the conventionally defined Bessel functions:

$$J_m(x) = (\frac{x}{2})^m \sum_0^\infty \frac{(-1)^r}{r! \Gamma(r+m+1)} (\frac{x}{2})^{2r}, \tag{A.12}$$

$$J_{-m}(x) = (\frac{x}{2})^{-m} \sum_0^\infty \frac{(-1)^r}{r! \Gamma(r-m+1)} (\frac{x}{2})^{2r}. \tag{A.13}$$

The denominator of Eqn. A.13 is infinite for negative integer arguments of the gamma function:

$$\Gamma(r-m+1) = \infty, \qquad r-m+1 = 0, -1, -2, \ldots,$$
$$r = m-1, m-2, \ldots, 0. \tag{A.14}$$

Changing the dummy summation index we obtain

$$J_{-m}(x) = (-1)^m J_m(x), \qquad m = 0, 1, 2, \ldots \tag{A.15}$$

Appendix B

Gamma function; recursion relations

The values of the following integral can be found easily for $\alpha > 0$, ([2])

$$\int_0^\infty e^{-\alpha x}dx = -\frac{1}{a}\left.e^{-\alpha x}\right|_0^\infty = \frac{1}{\alpha}. \tag{B.1}$$

After differentiating both side of this equation repeatedly with respect to α [2]

$$\int_0^\infty xe^{-\alpha x}dx = \frac{1}{\alpha^2},$$

$$\int_0^\infty x^2e^{-\alpha x}dx = \frac{2}{\alpha^3},$$

$$\int_0^\infty x^3e^{-\alpha x}dx = \frac{3!}{\alpha^4}.$$

or in general form

$$\int_0^\infty x^ne^{-\alpha x}dx = \frac{n!}{\alpha^{n+1}} \tag{B.5}$$

for $\alpha = 1$, we get

$$\int_0^\infty x^ne^{-x}dx = n! \tag{B.6}$$

For nonnegative n the followig integral is called the gamma Γ function.

$$\Gamma(n) = \int_0^\infty x^{n-1}e^{-x}dx = (n-1)!, \qquad n > 0. \tag{B.7}$$

and

$$\Gamma(n+1) = \int_0^\infty x^ne^{-x}dx = n! \qquad n > -1. \tag{B.8}$$

Integrating B.8 by parts, calling $x^n = u$, and $e^{-x}dx = dv$

$$\Gamma(n+1) = -x^ne^{-x}\Big|_0^\infty - \int_0^\infty (-e^{-x})nx^{n-1}dx$$

$$= n\int_0^\infty x^{n-1}e^{-x}dx = n\Gamma(n). \tag{B.9}$$

The equation

$$\Gamma(n+1) = n\Gamma(n) \tag{B.10}$$

is called the *recursion relation* for the Γ function.

Appendix C

Spherical harmonics

The explicit formulas for spherical harmonics [4] are

$$
Y_l^m(\theta, \phi) =
\begin{cases}
(-1)^m \sqrt{\frac{2l+1}{2} \frac{(l-m)!}{(l+m)!}} P_l^m(\cos\theta) \frac{e^{im\phi}}{\sqrt{2\pi}}, & m \geq 0, \\[2ex]
\sqrt{\frac{2l+1}{2} \frac{(l-|m|)!}{(l+|m|)!}} P_l^{|m|}(\cos\theta) \frac{e^{im\phi}}{\sqrt{2\pi}}, & m < 0, \\[2ex]
l = 0, 1, 2, \ldots, & m = -l, -l+1, \ldots, l-1, l.
\end{cases}
$$

and

$$
\begin{aligned}
P_l^m &= \frac{(1-x^2)^{m/2}}{2^l l!} \frac{\mathrm{d}^{l+m}}{\mathrm{d}x^{l+m}} (x^2-1)^l \\
&= \frac{(-1)^m (l+m)!}{2^l l! (l-m)!} \frac{1}{(1-x^2)^{m/2}} \frac{\mathrm{d}^{l-m}}{\mathrm{d}x^{l-m}} (x^2-1)^l.
\end{aligned}
\tag{C.1}
$$

The low order spherical harmonics from the above equations are as follows:

For $l = 0$

$$Y_0^0(\theta, \phi) = \frac{1}{\sqrt{4\pi}}$$

For $l = 1$

$$Y_1^1(\theta, \phi) = -\sqrt{\frac{3}{8\pi}} \sin\theta \mathrm{e}^{i\phi}$$

$$Y_1^0(\theta, \phi) = \sqrt{\frac{3}{4\pi}} \cos\theta$$

$$Y_1^{-1}(\theta, \phi) = \sqrt{\frac{3}{8\pi}} \sin\theta \mathrm{e}^{-i\phi}$$

For $l = 2$

$$Y_2^2(\theta, \phi) = \frac{1}{4}\sqrt{\frac{15}{2\pi}} \sin^2\theta \mathrm{e}^{2i\phi}$$

$$Y_2^1(\theta, \phi) = -\sqrt{\frac{15}{8\pi}} \sin\theta \cos\theta \mathrm{e}^{i\phi}$$

$$Y_2^0(\theta, \phi) = \frac{1}{2}\sqrt{\frac{5}{4\pi}} (3\cos^2\theta - 1)\mathrm{e}^{i\phi}$$

$$Y_2^{-1}(\theta, \phi) = \sqrt{\frac{15}{8\pi}} \sin\theta \cos\theta \mathrm{e}^{-i\phi}$$

$$Y_2^{-2}(\theta, \phi) = \frac{1}{4}\sqrt{\frac{15}{2\pi}} \sin^2\theta \mathrm{e}^{-2i\phi}$$

For $l = 3$

$$Y_3^3(\theta, \phi) = -\frac{1}{4}\sqrt{\frac{35}{4\pi}} \sin^3\theta \mathrm{e}^{3i\phi}$$

101

$$Y_3^2(\theta, \phi) = \frac{1}{4}\sqrt{\frac{105}{2\pi}} \sin^2\theta \cos\theta \mathrm{e}^{2i\phi}$$

$$Y_3^1(\theta, \phi) = -\frac{1}{4}\sqrt{\frac{21}{4\pi}} \sin\theta(5\cos^2\theta - 1)\mathrm{e}^{i\phi}$$

$$Y_3^0(\theta, \phi) = -\frac{1}{2}\sqrt{\frac{7}{4\pi}}(5\cos^2\theta - 3)\mathrm{e}^{i\phi}$$

$$Y_3^{-1}(\theta, \phi) = \frac{1}{4}\sqrt{\frac{21}{4\pi}} \sin\theta(5\cos^2\theta - 1)\mathrm{e}^{-i\phi}$$

$$Y_3^{-2}(\theta, \phi) = \frac{1}{4}\sqrt{\frac{105}{2\pi}} \sin^2\theta \cos\theta \mathrm{e}^{-2i\phi}$$

$$Y_3^{-3}(\theta, \phi) = \frac{1}{4}\sqrt{\frac{35}{4\pi}} \sin^3\theta \mathrm{e}^{-3i\phi}$$

Appendix D

ThermoC package

ThermoC [55] is a program package for the calculation of thermodynamic properties of pure fluid and binary fluid mixtures including phase equilibria, with arbitrary equations of state (EOS) and mixing rules. This package is able to administrate a large number of equations of state The package programs can be divided into three classes:

1. main programs, which are independent of the equations of state and the models used; and calculate the properties,

2. model-dependent subroutines, containing equations of state or mixing rules,

3. model-independent subroutines, containing universal thermodynamic relations, mathematical codes which are used by main programs.

By linking the model-independent programs with the model-dependent code, executable programs for a thermodynamic model are obtained.

The program package contains the following directories:

program package directories	
bin:	executables
ideal:	caloric properties of the perfect gas
include:	header files
lib:	object file archives
main:	main programs
models:	model-specific subroutines
solid:	sublimation or melting curve data
thsub:	model-independent subroutines
spinodal1	spinodals
math:	mathematical subroutines

The following main programs are available for pure substances:

	programs for pure compounds
bfmgr1:	maintains data base files (pure compounds)
check1:	consistency test for user-supplied
	subroutine moduies
ffe1:	vapour pressure curve of a pure fluid
reduc1:	reads experimental data of pure fluids, calculates
	EOS parameters, and writes them to a data base file
sfe1:	sublimation pressure curve of a pure fluid
vir1:	virial coefficients
xth1:	thermodynamic properties of a single phase

The following main programs are available for binary mixtures:

	programs for binary mixtures
bfmgr2:	maintains data base files (binary mixtures)
crit2:	critical curves of binary mixtures
ffe2:	VLE, LLE, for binary mixtures
mix2-Hp:	temperature and volume change upon
	isenthalpic-isobaric
	mixing of two pure fluids
mix2-HS:	temperature and volume change upon
	isenthalpic-isentropic
	mixing of two pure fluids
reduc2:	EOS parameter estimation for binary mixtures
sfe2:	SLE, SGE for binary mixtures
spinodal2:	spinodals of binary mixtures
xth2:	single phase properties of binary mixtures
	(including excess properties)

List of equations of state in thermoc package:

	programs for binary mixtures
CSRK	Carnahan–Starling repulsion + Redlich–Kwong attraction
CSvdW	Carnahan–Starling repulsion + van der Waals attraction
D1	Deiters
D1A	Deiters with chain association
D1-qu	Deiters EOS + new quantum correction
IUPAC-N2	IUPAC reference equation for nitrogen
IUPAC-CO2	IUPAC reference equation for carbon dioxide
IUPAC-CH4	IUPAC reference equation for methane
Mxw2RK	soft sphere repulsion + Redlich–Kwong attraction
Mxw2vdW	soft sphere repulsion + van der Waals attraction
Nicolas	Nicolas (BWR-type equation for the Lennard–Jones fluid
PR	Peng–Robinson
RK	Redlich–Kwong
RKS	Redlich–Kwong–Soave
SL	Sanchez–Lacombe
SPHCT	Simplified Perturbed Hard Chain
TBS	Trebble–Bishnoi–Salim
vdW	van der Waals
YKD4vdW	Yelash–Kraska–Deiters quartic + van der Waals attraction

Appendix E

Simulation

Table E.1:

ab initio potentials (μE_h) for the neon dimer.

R (Å)	avqz	av5z	av45z
2.250	3635.34	3502.53	3363.19
2.500	854.25	787.66	717.80
2.750	81.52	50.78	18.53
3.000	-91.51	-107.72	-124.73
3.075	-102.80	-116.27	-130.40
3.100	-104.59	-117.34	-130.72
3.125	-105.50	-117.63	-130.36
3.250	-102.22	-111.79	-121.83
3.500	-79.24	-85.35	-91.76
3.750	-56.11	-59.92	-63.92
4.000	-38.87	-41.19	-43.62
4.500	-18.96	-19.84	-20.76
5.000	-9.78	-10.20	-10.64

Table E.2: Parameters of fitting for the neoen–neon potentials.

Parameter	avtz+(332)	av5z	av45z
A (E_h)	78.52	68.59	75.40
α (a_0^{-1})	2.13371	2.09504	2.16774
β (a_0^{-2})	-.035	-.040	-.027
b (a_0^{-1})	1.88	1.65	1.86
C_6 ($E_h a_0^6$)	6.96	6.01	6.08
C_8 ($E_h a_0^8$)	49.87	9.80	114.08
C_{10} ($E_h a_0^{10}$)	2393.96	6832.96	2008.32

Table E.3:

GEMC simulation results of neon using the av45z plus AT potentials.

T/K	ρ/kgm^{-3}	U/Jmol^{-1}	p/MPa	μ/Jmol^{-1}	H/Jmol^{-1}
27(g)	5.0(4)	-10(9)	0.053(4)	-2175(17)	208(3)
27(l)	1294(4)	-1796(7)	0.17(32)	-1849(103)	-1794(8)
30(g)	13(1)	-29(3)	0.15(2)	-2241(23)	206(5)
30(l)	1234(10)	-1692(17)	-0.002(458)	-2127(93)	-1693(19)
32(g)	21(3)	-45(7)	0.26(3)	-2304(29)	196(11)
32(l)	1188(7)	-1614(11)	0.31(16)	-2285(61)	-1609(12)
35(g)	40(3)	-78(6)	0.50(3)	-2407(17)	172(9)
35(l)	1126(7)	-1513(10)	0.64(16)	-2385(39)	-1502(9)
37(g)	62(6)	-116(11)	0.75(6)	-2473(18)	130(16)
37(l)	1080(4)	-1440(7)	0.77(20)	-2484(26)	-1426(6)
40(g)	97(4)	-173(7)	1.18(3)	-2608(7)	73(13)
40(l)	997(12)	-1320(19)	1.22(27)	-2603(14)	-1296(18)
42(g)	155(4)	-267(7)	1.67(3)	-2676(5)	-49(10)
42(l)	938(17)	-1237(23)	1.82(36)	-2708(29)	-1199(24)

Bibliography

[1] C. W. Sherwin, *Introduction to Quantum Mechanics,* Holl, Reinhart and Winston, New York 1959.

[2] M. L. Boas, *Mathematical Methods in the Physical Sciences,* John Wiley & Sons, New York 1983.

[3] H. W. Wyld, *Mathematical Methods for Physics* (The Benjamin/ Cummings Publishing Company, California 1976).

[4] G. Arfken, *Mathematical methods for physicists,* Academic Press New York 1966.

[5] Edited by M. Abramowitz and I. A. Stegun, *Handbook of Mathematical Functions,* Dover Publications, New York 1964.

[6] I. N. Levin, *Quantum Chemistry,* Prentice-Hall, New Jersey 1991.

[7] D. A. McQuarrie, *Statistical Mechanics,* Harper & Row, New York 1976.

[8] T. M. Reed, K. E. Gubbins, *Applied Statistical Mechanics, Thermodynamic and Transport Properties of Fluids,* McGraw-Hill, Kogakusha Tokyo 1973.

[9] H. B. Callen, *Thermodynamics and an Introduction to Thermostatics,* John Wiley & Sons, New York 1985.

[10] O. Redlich and J. N. S. Kwong, *Chem. Rev.* **44**, 233 (1949).

[11] G. Soave, *Chem. Eng. Sci.,* **27**, 1197 (1972).

[12] D. Y. Peng and D. B. Robinson, *Ind. Eng. Chem. Fundam.* **15**, 59 (1976).

[13] G. G. Fuller, *Ind. Eng. Chem. Fundam.* **15**, 254 (1976).

[14] S. I. Sandler, *Models for Thermodynamic and Phase Equilibria Calculations,* Marcel Dekker, New York 1994.

[15] G. Schmidt and H. Wenzel, *Chem. Eng. Sci.* **35**, 1503 (1980).

[16] A. Harmens, and H. Knapp, *Ind. Eng. Chem. Fundam.,* **19**, 291 (1980).

[17] W. A. Kubic, *Fluid Phase Equilib.,* **9**, 79 (1982).

[18] N. C. Patel, and A. S. Teja, *Chem. Eng. Sci.,* **37**, 463 (1982).

[19] Y. Adachi, B. C. Lu, and H. Sugie, *Fluid Phase Equilib.,* **13**, 133 (1983).

[20] Y. Adachi, B. C. Lu, and H. Sugie, *Fluid Phase Equilib.,* **11**, 29 (1983)

[21] R. Stryjek, and J. H Vera, *Can. J. Chem. Eng.,* **64**, 323 (1986).

[22] J. M. Yu, and B. C.-Y. Lu, *Fluid Phase Equilib.,* **34**, 1 (1987).

[23] M. A. Trebble, and P. R. Bishnoi, *Fluid Phase Equilib.,* **40**, 1 (1987).

[24] J. Schwartzentruber, and H. Renon, *Fluid Phase Equilib.,* **52**, 127 (1989).

[25] E. A. Guggenheim, *Mol. Phys.,* **9**, 199 (1965).

[26] N. F. Carnahan, and K. E. Starling, *J. Chem. Phys.,* **51**, 635 (1969).

[27] R. L. Scott, *Physical Chemistry, an Advanced Treatis, Vol. 8A, Liquid State*, H. Eyring, D. Henderson, and W. Jost, eds., Academic Press, New York 1971.

[28] T. Boublík, *Ber. Bunsenges. Phys. Chem.,* **85**, 1038 (1981).

[29] R. Clausius, *Ann. Phys. Chem.,* **9**, 337 (1881).

[30] D. J. Berthelot, *J. Phys.,* **8**, 263 (1899).

[31] J. V. Sengers, R. F. Kayser, C. J. Peters, and H. J. White, Jr. in *Equations of State for Fluids and Fluid Mixtures, part I Experimental Thermodynamics, volume V,* Elsevier Science, Netherlands 2000.

[32] J.-M. Yu, Y. Adachi, and, B. C.-Y. Lu, *Equations of State – Theories and Applications*, K. C. Chao, and R. L. Robinson Jr., eds., ACS Symposium Ser.; **300**, 537 (1986).

[33] Y. S. Wie, and R. J. Sadus, *AIChE J.,* **46**, 169 (2000).

[34] S. Malanowski, and A. Anderko, *Modeling Phase Equilibria, Thermodynamic Background and Practical Tools,* John Wiley & Sons, NewYork 1992.

[35] M. M. Abbot, *Adv. Chem. Ser.,* **182**, 47 (1979).

[36] G. M. Wilson, *Adv. Cryog. Eng.,* **9**, 168 (1964).

[37] R. C. Reid, J. M. Prausnitz, and B. E. Poling, *The Properties of Gases and Liquids, 4th ed.*, McGraw-Hill, New York 1987.

[38] R. C. Reid, J. M. Prausnitz, and B. E. Poling, *The Properties of Gases and Liquids, 3th ed.*, McGraw-Hill, New York 1977.

[39] TRC *Thermodynamic tables, Hydrocarbons*, Engineering experiment station, Texas A & M University, College Station.

[40] TRC *Thermodynamic tables, Non–Hydrocarbons*, Engineering experiment station, Texas A & M University, College Station.

[41] P. Watson, M. Cascella, D. May, S. Salerno, and D. Tassios, *Fluid Phase Equil.*, **27**, 35 (1986).

[42] R. W., Zwanzig, *J. Chem. Phys.*,22, 1420 (1954).

[43] P. C. Hemmer, M. Kac, and G. E. Uhlenbeck, *J. Math. Phys.* , **5**, 60 (1964).

[44] J. A. Barker, and D. Henderson, *Adv. Phys. Chem.* , **23**, 233 (1972).

[45] Y. Adachi, and H. Sugie, *Fluid Phase Equilib.* , **28**, 103 (1986)

[46] A. Z. Panagiotopoulos, and R. C. Reid, *Equations of State– Theories and Applications*, K. C. Chao, and R. L. Robinson Jr., eds., ACS Symps Ser.; 300, 571 (1986).

[47] R. Stryjek, and J. H Vera, *Can. J. Chem. Eng.*, **64**, 334 (1986).

[48] J. Schwartzentruber, F. Galivel, Solastiouk, and H. Renon, *Fluid Phase Equilib.*, **38**, 217 (1987).

[49] R. Sandoval, G. Wilkzek, and J. H. Vera, *Fluid Phase Equilib.*, **52**, 119 (1989).

[50] Ulrich K. Deiters, *Chem. Eng. Sci.*, 36, 1139 (1981) .

[51] Ulrich K. Deiters, *Chem. Eng. Sci.*, 36, 1147 (1981) .

[52] Ulrich K. Deiters, *Chem. Eng. Sci.*, 37, 855 (1982) .

[53] Ulrich K. Deiters, *Fluid Phase Equil.*, 10, 173 (1983) .

[54] Ulrich K. Deiters, *Fluid Phase Equil.*, 13, 109 (1983) .

[55] Ulrich K. Deiters, *Chem. Eng. Techno.*, 23, 581 (2000) .

[56] Ulrich K. Deiters, *Fluid Phase Equil.*, 33, 267 (1987) .

[57] Ulrich K. Deiters, *Fluid Phase Equil.*, 48, 185 (1989) .

[58] B. P. Singh, and S. K. Sinha, *J. Chem. Phys.*, **68**, 562 (1978) .

[59] B. P. Singh, and S. K. Sinha, *J. Chem. Phys.*, **69**, 2709 (1978) .

[60] S. D. Hamann, *Trans. Faraday Soc.*, **48**, 303 (1952) .

[61] S. D. Hamann, *Trans. Faraday Soc.*, **49**, 711 (1953) .

[62] J. M. H. Levelt, and R. P Hurst, *J. Chem. Phys.*, **32**, 96 (1960) .

[63] M. A. Hooper, and S. Nordholm, *Aust. J. Chem.*, **33**, 2029 (1980) .

[64] J. Kohlbruch, *Entwicklung einer Zustandsgleichung realer Fluide unter besonderer Berücksichtigung der Quanteneffekte*, (Shaker Verlag 1997) .

[65] A. E. Nasrabad, and U. K. Deiters, in peparation.

[66] A. Z. Panagiotopoulos, *Mol. Phys.*, **61**, 813 (1987) .

[67] B. M. Axilrod, and E. Teller, *J. Chem. Phys.*, **11**, 299 (1943) .

[68] K. Leonhard, and U. K. Deiters, *Mol. Phys.*, **98**, 1603 (2000) .

[69] T. Korona, L. Wiliams, R. Bukowski, B. Jeziorski, and K. Szalewicz, *J. Chem. Phys.*, **106**, 5109 (1997).

[70] S. M. Cybulski and R. R. Toczylowski, *J. Chem. Phys.,*, **111**, 10520 (1999).

[71] K. T. Tang and J. P. Toennies, *J. Chem. Phys.,* **80**, 3726 (1984).

Lebenslauf

Name:	Laghaei
Vorname:	Rozita
Geschlecht:	Weiblich
Geburstsdatum:	14 Jan. 1971
Geburstort:	Teheran (IRAN)
Familienstand:	Ledig

Ausbildung:

Promotion:	Von Sommer Semester 2001 - Feb. 2003
	Physikalische Chemie
	Universität zu Köln
	Deutschland

Betreuer:	Prof. Dr. U. K. Deiters
Titel meiner	"Calculation of phase equilibria for
Dissertation:	quantum fluids at high pressure "

M.Sc. (Diplom):	Sep.1994 - Feb.1998
	Physikalische Chemie
	Universität zu Teheran
	Iran
Betreuer:	Prof. Dr. Ali Maghari
Titel meiner	" The Extended Kinetic Theory
Diplom Arbeit:	of Dense Fluids "

B.SC.	Sep.1990 - Jul.1994
	Chemie
	Universität zu Teheran
	Iran

Erklärung

"Ich versichere, daß ich die von mir vorgelegte Dissertation selbständig angefertigt, die benutzten Quellen und Hilfsmittel vollständig angegeben und die Stellen der Arbeit-einschließ lich Tabellen, Karten und Abbildungen -, die anderen Werken im Wortlaut oder dem Sinn nach entnommen sind, in jedem Einzelfall als Entlehnung kenntlich gemacht habe; daß diese Dissertation noch keiner anderen Fakultät oder Universität zur Prüfung vorgelegen hat; daß sie - abgesehen von unten angegebenen Teilpublikationen - noch nicht veröffentlicht worden ist sowie, daß sich eine solche Veröffentlichung vor Abschluß des Promotionsverfahrens nicht vornehmen werde. Die Bestimmungen dieser Promotionsordnung sind mir bekannt. Die von mir vorgelegte Dissertation ist von Professor Dr. U. K. Deiters betreut worden."

Name: Rozita Laghaei

Datum............................   Unterschrift...